

VERTICAL TEMPERATURE AND MOISTURE PROFILES
FROM SATELLITE RADIANCE MEASUREMENTS

EDUCATIONAL MODULES FOR
THE ATMOSPHERIC SCIENCES

Space Science and Engineering Center
University of Wisconsin-Madison
1225 West Dayton Street
Madison, Wisconsin 53706

Contributions by

T. H. Achtor
D. R. Johnson

D. R. Johnson, Project Director

The development of this module for atmospheric science education through use of video systems has been supported by the National Science Foundation under Grants SED79-19005 and ATM 8217164.

Any opinions, findings, and conclusions or recommendations expressed in this publication are those of the author(s) and do not necessarily reflect the views of the National Science Foundation.

August 1984

TABLE OF CONTENTS

	Page
i Table of Contents	i
ii List of Symbols	iii
iii List of Figures	v
I. Introduction	1
II. Description of the Module Contents	2
III. Academic Considerations	4
IV. Development of Satellite Technology for Sounding the Atmosphere	5
A. Background	5
B. Instrumentation	5
C. Sounding Techniques	7
V. Fundamental Physical Principles for Remote Sensing	8
A. Fundamental Concepts of radiation	8
B. Atmospheric effects on radiation	15
VI. Radiative Transfer	21
VII. Linearization of the Radiative Transfer Equation	29
VIII. Temperature Profile Solutions to the Radiative Transfer Equation	32
A. Iterative Methods (Direct Solution of the Radiative Transfer Equation)	35
B. Matrix Methods (Indirect Solution of the Radiative Transfer Equation)	37
IX. Temperature Profile Solutions for Cloud Covered Conditions	39
X. Moisture Profile Solutions to the Radiative Transfer Equation	44
XI. Current Instrumentation for Vertical Soundings	48

Table of Contents (Cont.)

	Page
XII. Videocassette Case Summaries	54
A. 26 April 1982: a severe weather event over the southeast United States	55
B. 12-13 September 1982: Hurricane Debby	60
XIII. References	66
Appendix A: Module Evaluation	74
A: Instructor Evaluation Form	75
B: Student Evaluation Form	81
Appendix B: Videocassette Technical Guide	85

A. List of Symbols

T_b	equivalent blackbody (brightness) temperature
λ	wavelength
T	temperature
c_1	a constant in Planck's Law equal to $3.74 \times 10^{-16} \text{ Wm}^2$
c_2	a constant in Planck's Law equal to $1.44 \times 10^{-2} \text{ m K}$
ν	wavenumber
I_λ	upwelling monochromatic radiance intensity as a function of wavelength
I_s	upwelling monochromatic radiance intensity from earth's surface as a function of wavelength
R	observed (measured) radiance
a	absorbed radiation
r	reflected radiation
τ	transmitted radiation
e	emissivity
θ	viewing angle
B_λ	Planck blackbody monochromatic intensity of radiation as a function of wavelength
B_ν	Planck blackbody monochromatic intensity of radiation as a function of wavenumber
z	geopotential height
k	coefficient of absorption
ρ	density of the atmosphere
t	time

List of Symbols (cont.)

- p pressure
- q mixing ratio of absorbing constituent
- g gravity
- u optical path length
- o subscript to denote initial estimates of variables in Taylor series expansion

B. List of Figures

- Fig. 1 Electromagnetic spectrum with atmospheric transmission characteristics.
- Fig. 2 Planck function for characteristic earth/atmosphere temperatures.
- Fig. 3 Planck function distribution (terrestrial) with actual transmittance.
- Fig. 4 Atmospheric effects on radiation.
- Fig. 5 Schematic of the layer solution of the radiative transfer equation.
- Fig. 6 Radiation to space in the 15 μm region of the spectrum.
- Fig. 7 Weighting functions for TOVS IR channels.
- Fig. 8 Scan geometry for polar orbiting satellites.
- Fig. 9 Weighting functions for TOVS microwave channels.
- Fig. 10 Weighting functions for TOVS water vapor channels.

Maps for 26 April 1982

- Fig. 11 1200 GMT 500 mb geopotential height and temperature.
- Fig. 12 1800 GMT surface pressure, fronts and dewpoints $> 15^{\circ}\text{C}$.
- Fig. 13 VAS Total Totals Stability Index.
- Fig. 14 2035 GMT NMC radar depiction.
- Fig. 15 Tornado reports.

Maps for 15-16 September 1982

- Fig. 16 Storm track for Hurricane Debby.
- Fig. 17 Pressure and wind trace for Hurricane Debby.
- Fig. 18 VAS and special radiosonde network 850 mb temperatures.

I. INTRODUCTION

This educational module, designed for senior-graduate level coursework, investigates the physical and mathematical basis for obtaining vertical temperature and moisture profiles of the atmosphere from satellite borne remote sensors. The objectives of the module are to: 1) review the theoretical background for this problem of indirect sensing, 2) discuss mathematical solutions, 3) investigate the application of these solutions to vertically sounding the earth's atmosphere, and 4) display results achieved using remote sensing data from geosynchronous and polar orbiting satellites. This module utilizes results obtained from an interactive videocomputer to aid in this study.

The use of satellite derived profiles of temperature and moisture is important for atmospheric research and forecasting. Such data increase spatial and temporal resolution of atmospheric information and provide a global data network for the benefit of many meteorological endeavors. The topic merits study by meteorologists in order to understand the complexity involved in obtaining accurate profiles of temperature and moisture from remote sensors and to learn the unique characteristics of the data.

Observations of the atmospheric temperature and moisture distributions derived from satellite data are a relatively new source of information to the atmospheric sciences. Instrumentation onboard satellites and methods of calculating meteorological parameters are constantly being improved by ongoing research. Thus, some parts of the module may become outdated. However, the physical basis of sounding the

atmosphere which is summarized in this module will likely remain unchanged.

II. DESCRIPTION OF THE MODULE CONTENTS

The utilization of interactive video computers in atmospheric science has enabled scientists to work effectively with meteorological satellite data on a real time basis. Satellite derived images and meteorological fields can be combined to estimate the four dimensional structure and evolution of the atmosphere for research and forecasting. The display of this capability through videocassettes provides insight into the techniques and potential of this type of system. The McIDAS (Man-computer Interactive Data Access System) videocomputer, used to produce the videocassette, has the capability of superimposing analyzed fields of meteorological data over satellite imagery and forming a time sequence. The fields may be derived from surface and radiosonde data, from satellite derived information, or from a combination of these sources. In addition to satellite images with superimposed graphics, other physical and mathematical concepts can be displayed using the McIDAS graphics capability. Examples of these products are contained in this educational module.

This module consists of two components. The first comprises a 55-minute videocassette featuring sequences of satellite imagery and background information for obtaining vertical temperature and moisture profiles by remote sensing of the atmosphere. The videocassette contains examples of sounding retrievals and results from research produced using

the McIDAS videocomputer at the University of Wisconsin Space Science and Engineering Center (SSEC). A videocassette technical guide outlines the sequence of images and graphics and provides technical information.

This manual, the second component of the module, contains: 1) a description of the module contents and suggestions for its utilization, 2) a review of the physical and mathematical bases for obtaining vertical atmospheric soundings, 3) a discussion of past and present weather satellites which provide the raw data, 4) a brief discussion of the synoptic situations used as examples in the videocassette, 5) a list of references offering greater detail on subjects covered in this module, and 6) a questionnaire in which the instructor and students can evaluate the educational value of the module and offer suggestions for improvement. The following list details the chronological sequence of the videocassette. A more complete listing is contained in the Videocassette Technical Guide (Appendix B).

VIDEOCASSETTE CONTENTS

1. Introduction
2. Satellite characteristics
3. Physical basis of remote soundings
4. Satellite instrument characteristics
5. Solutions to the radiative transfer equation
6. Examples of the use of satellite soundings

III. ACADEMIC CONSIDERATIONS AND UTILIZATION OF THE MODULE

The module is best utilized in conjunction with a series of detailed lectures that present physical and mathematical principles of indirect sensing. While the academic level of this module is directed towards senior-graduate level coursework, the module has been structured to permit utilization over a broader range of academic levels. Prerequisite levels are familiarity with atmospheric radiation theory, elementary differential equations and matrix algebra. Statistical methods are also employed in the solutions. The depth of the mathematical treatment can be varied considerably in the module utilization. However, in order to gain an overall understanding of the problem, a familiarity with the above subjects is necessary. It is possible to deal briefly with the section on mathematical solutions and focus on the research and forecasting aspects of the technology. Reference material may be used in conjunction with the module to provide more depth and emphasis in specific areas.

Within the series of lectures dealing with the subject, segments of the videocassette should be examined and discussed in conjunction with the lecture material. Attempts to show the videocassette and discuss the problem of remote sensing in one sitting, without prior study, will create a difficult experience for the student due to the complexity of the material.

IV. DEVELOPMENT OF SATELLITE TECHNOLOGY FOR SOUNDING THE ATMOSPHERE

A. Background

The development of technology to place earth orbiting satellites into space brought forth a corresponding development in engineering and the atmospheric sciences to design and deploy satellite instrumentation for indirect sensing of temperature and moisture profiles of the atmosphere. A theoretical basis for this endeavor already existed. Soon after Schuster, in 1905, conceived the radiative transfer equation, the concept was applied to the study of the spectra of the stars and the sun. Applications of radiance measurements to obtain profiles of the earth's atmosphere are much simpler, since the composition of the atmosphere is known with considerable precision. King (1950), Kaplan (1959) and Wark (1961) proposed the inference of atmospheric profiles from satellite measurements of infrared radiation. They suggested the application of the radiative transfer equation to satellite measurements over narrow intervals in the 15 μm absorption band of carbon dioxide (CO_2). While groups of scientists worked to design more sophisticated instrumentation for satellite measurements, others studied the physical-mathematical basis for obtaining accurate solutions.

B. Instrumentation

The Nimbus 3 and 4 satellites (circa 1969) carried the first versions of the Satellite Infrared Spectrometer (SIRS) and the Infrared Interferometer Spectrometer (IRIS). The two differed principally in the bandwidth resolution of the measurement. Both measured upwelling

radiation from several narrow spectral intervals in the 15 μm infrared absorption band of the electromagnetic spectrum. These intervals were located from the center of the absorption band out to the wings or edges of the band. The combined effect of the location of an interval within the band and magnitude of the observed upwelling radiation supplied information about the temperature of a certain atmospheric layer. Several well chosen intervals within the absorption band provide sufficient detail to calculate the temperature at a number of levels that comprise the vertical profile.

The Nimbus 5 spacecraft (1972) carried the Infrared Temperature Profile Radiometer (ITPR), a new generation of instrumentation designed to increase the horizontal resolution of the measurements. In areas of partial cloud cover the relatively low spatial resolution of the SIRS instrument resulted in little or no information about the thermal structure of the atmosphere below cloud top, since clouds absorb upwelling infrared radiation. The problem of partial cloudiness within a satellite field of view stems from the condition that a given observation is neither representative of radiation emitted from the cloud free or cloud covered portion of the atmosphere. Consequently, realistic vertical profiles could not be retrieved without knowledge of the fractional area of the satellite field of view covered by clouds. The ITPR was designed with a higher spatial resolution to resolve these problems. Techniques were developed that compared adjacent fields of view to eliminate the influence of clouds. The Vertical Temperature Profile Radiometer (VTPR) onboard early operational NOAA satellites

utilized this concept. Nimbus 5 also carried the first microwave sounding device, NEMS (Nimbus E Microwave Sounder). Since small water droplets do not attenuate microwave radiation, this instrument provides temperature information below cloud level.

A multi-band infrared sensor was adopted for use on the Nimbus 6 (1975) and later polar orbiting satellites. The High resolution Infrared Radiation Sounder (HIRS) observes the 4.3 μm , as well as the 15 μm CO₂ absorption bands in several spectral intervals simultaneously. The two absorption bands each contain unique characteristics that result in improved temperature profiling accuracy. A scanning capability was added to the microwave instrument with the Scanning Microwave Spectrometer (SCAMS).

C. Sounding techniques

Throughout the period of instrument development, the need for improving the quality of atmospheric profiles of temperature and moisture from satellite radiance data has existed. Prior to the early Nimbus launches, Wark and Fleming (1966) detailed the problems. For a direct physical solution, an integral form of the radiative transfer equation must be used. The spectral radiance data must be linearized and the transmittance must be calculated from models and expressed in terms of weighting functions. Since the matrix solution involves a nonlinear, second order differential equation with no exact solution, the problem is non-unique and a number of possible solutions exist. Thus, due to the inherent mathematical instability of the radiative transfer equation,

sophisticated "fine tuning" of the data or stochastic methods of solution must be utilized.

Methods of solution are of two types, physical and statistical. An example of the former is an iterative approach based on the physics of the radiative transfer equation which uses a first guess profile to converge on the "best" result. An example of the latter is the method of discriminant and/or regression statistics which may completely bypass the physics of the radiative transfer equation and obtain a purely statistical solution. Solutions of this type produce a best fit profile to the radiance data based on prior information. Forms of both methods of solution as well as combinations of the two are currently in use.

V. FUNDAMENTAL PHYSICAL PRINCIPLES FOR REMOTE SENSING

This section reviews radiation principles fundamental to remote sensing. Following an introduction to the electromagnetic spectrum, Planck's law and its corollaries which govern basic concepts of radiation are discussed. With this background and the principle of energy conservation, the effects of the earth's atmosphere upon terrestrial radiation are reviewed. Finally, methods for obtaining atmospheric temperature and moisture profiles from the emitted spectrum of terrestrial radiance are presented.

A. Fundamental concepts of radiation

Fundamental to the theory of electromagnetic radiation are the concepts of an energy spectrum (Fig. 1) and energy transfer by wave propagation. In a vacuum all wavelengths travel at the same speed,

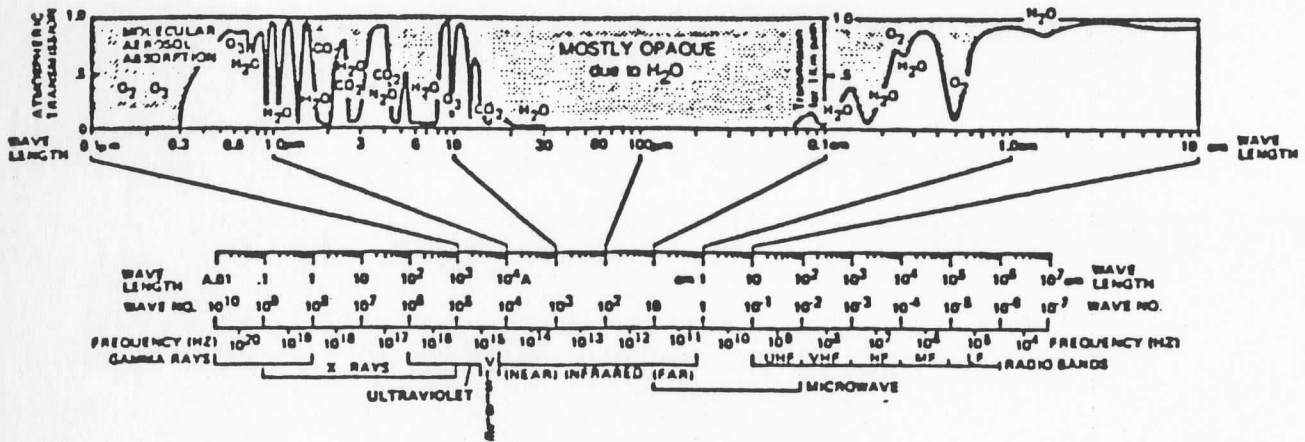


Figure 1: Electromagnetic spectrum showing atmospheric transmission characteristics and major absorbing constituents.

approximately $3.0 \times 10^8 \text{ ms}^{-1}$. Within the earth's atmosphere, electromagnetic radiation is affected by selective absorption, re-emission, and reflection due to interaction of the radiation beam with molecules of various atmospheric constituents. The radiative flux associated with electromagnetic waves serves to transfer energy between space, different layers of the atmosphere and the earth's surface.

1. Planck's Law

The fundamental laws governing electromagnetic radiation and radiative transfer utilize the concept of a blackbody. The amount of radiation emitted by a blackbody is uniquely determined by its temperature. This hypothetical body is comprised of a sufficient number of molecules absorbing and emitting electromagnetic radiation in all areas of the electromagnetic spectrum such that all incident radiation in all wavelength bands is completely absorbed from all directions. In turn the emission of the body at all wavelengths is in equilibrium with its absorption. The distribution of emitted radiation for a blackbody with temperature T is described by Planck's law. The Planck function, B_λ , the monochromatic intensity of radiation as a function of wavelength λ , is given by

$$B_\lambda = \frac{c_1}{\lambda^5 [\exp(c_2/\lambda T) - 1]} \quad (1)$$

where c_1 and c_2 are constants respectively equal to $3.74 \times 10^{-16} \text{ Wm}^2$ and $1.44 \times 10^{-2} \text{ m K}$.

The wavelength of a radiation beam is the distance between two consecutive wave crests or troughs. Wavenumber, the reciprocal of wavelength,

$$\nu = \frac{1}{\lambda}$$

is the number of wavelengths per unit length. With the relations

$$dv = \left| \frac{\partial v}{\partial \lambda} \right| d\lambda = \frac{1}{\lambda^2} d\lambda$$

and

$$B_\lambda d\lambda = B_\lambda \left| \frac{\partial \lambda}{\partial v} \right| dv = B_\nu dv,$$

the distribution of monochromatic intensity of radiation expressed by Planck's Law in terms of wavenumber is

$$B_\nu = \frac{c_1 \nu^3}{[\exp(c_2\nu/T)-1]} \quad (2)$$

The blackbody spectrum of radiation for characteristic earth temperature is shown in Fig. 2. The distribution shows that the intensity of radiation at shorter wavelengths (higher wavenumbers) is more strongly dependent on the temperature of the emitting body than at longer wavelengths (smaller wavenumbers). At relatively short wavelengths, for example in the near infrared, the relationship between radiance and temperature is exponential (Wein law of radiation), while a nearly linear relationship exists in the far infrared and microwave portion of the spectrum (Rayleigh-Jeans law of radiation). Figure 2 shows that the

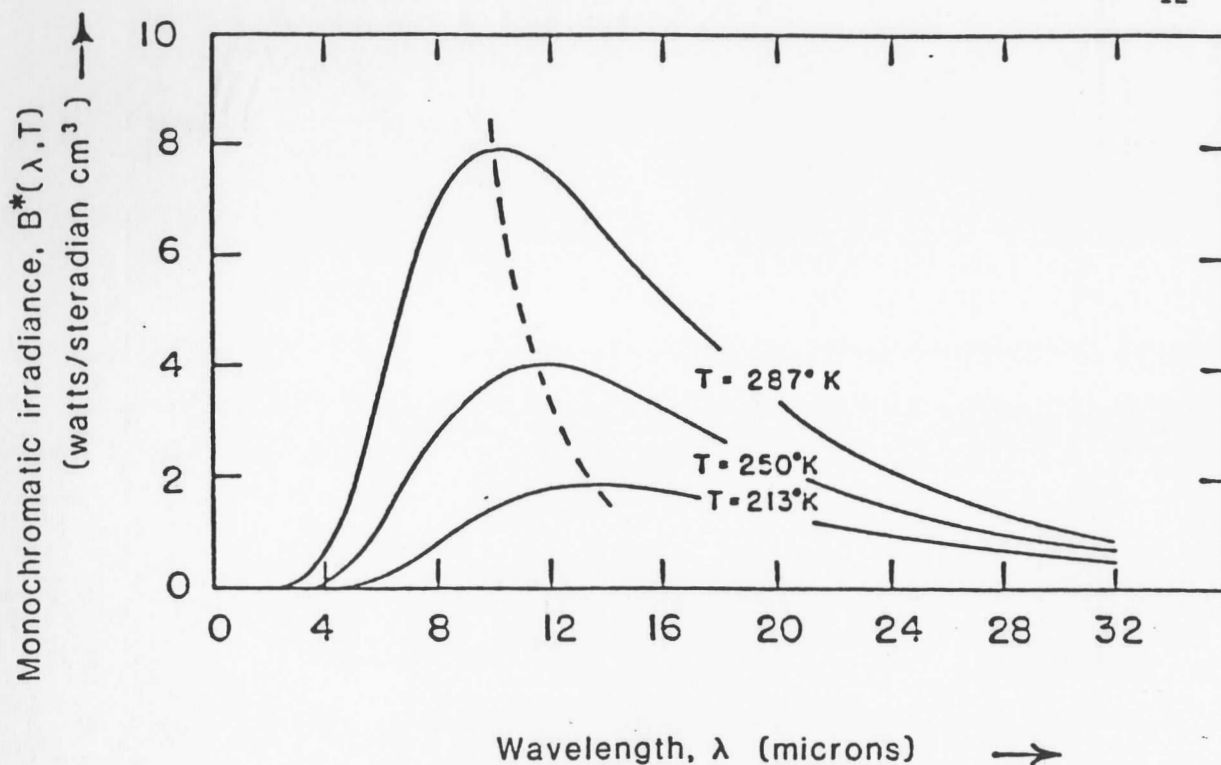


Figure 2: Black body distribution of energy for temperatures corresponding to the mean surface temperature of the earth, the mean atmospheric temperature, and a characteristic tropopause temperature.

total amount of radiation emitted from a source and its wavelength of maximum emission is a function of the temperature of the emitting body. The figure also indicates that the wavelength of maximum emission described by the Planck function shifts toward shorter wavelengths with increasing temperature. The wavelength of maximum emission (λ_m) determined by differentiating the Planck function with respect to wavelength and equating the result to zero (i.e., determining where the slope is zero) is given by

$$\lambda_m[\mu\text{m}] = \frac{2897}{T} . \quad (3)$$

This equation, called Wien's displacement law, determines the wavelength of maximum emission from the temperature of the blackbody. The sun radiates very nearly as a blackbody with a radiative temperature of approximately 5750 K. Using Wien's displacement law the maximum emission of radiation from the sun occurs near the center of the visible portion of the spectrum at 0.5 μm . The effective radiative temperature of the earth is approximately 255 K which corresponds to a maximum of emission in the infrared portion of the spectrum at 11.4 μm . The actual spectrum of radiation emitted by the earth's surface and atmosphere when compared with Planck's blackbody distribution of radiation in Fig. 3 shows the significant departures due to the variable effects of absorption and reemission by component gases in the atmosphere.

To account for these variations in remote sensing of the atmosphere, an effective radiative or equivalent blackbody temperature is defined

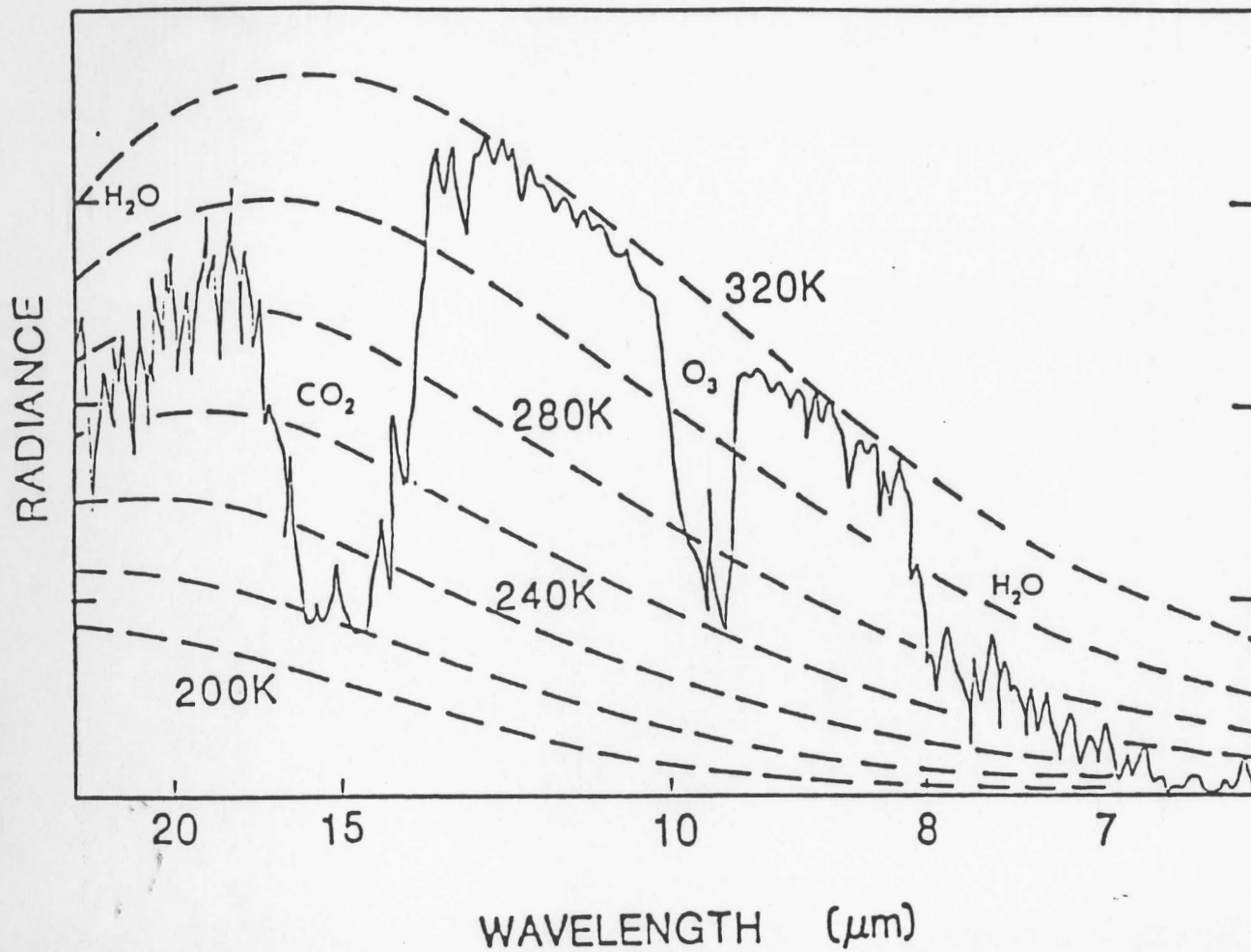


Figure 3: Planck distribution of emitted radiation for selected effective black body temperatures (dashed) and a sample observed emission spectrum (solid) with principal absorbing constituents.

as a function of wavelength (or wavenumber). A solution for the temperature from the Planck function from (2) yields

$$T(\nu) = \frac{c_2 \nu}{\ln [1 + c_1 \nu^3 / B_\nu]} . \quad (4)$$

When the measured radiance at a particular wavenumber is used to determine B_ν in (4), the temperature is defined to be the effective radiative or equivalent blackbody temperature, sometimes called the brightness temperature T_b . This relationship is frequently used to express a satellite radiance measurement by its equivalent blackbody temperature. The difference between the actual and the equivalent blackbody temperatures is due to the variable emissivity of the radiating body as a function of wavenumber and the effects of the atmosphere. In such a case no single temperature T_b may be used to characterize the overall spectrum of radiation.

B. Atmospheric effects on radiation

A radiation beam propagating through the atmosphere interacts with molecules in its path. Radiation incident upon a non-opaque atmospheric layer is either absorbed (a), reflected (r), or transmitted (τ) (see Fig. 4). Through the conservation of energy, this relation is expressed as

$$a(\lambda) + r(\lambda) + \tau(\lambda) = 1 . \quad (5)$$

If the atmosphere were completely transparent in a certain wavelength no absorption or reflection would occur and all terrestrial

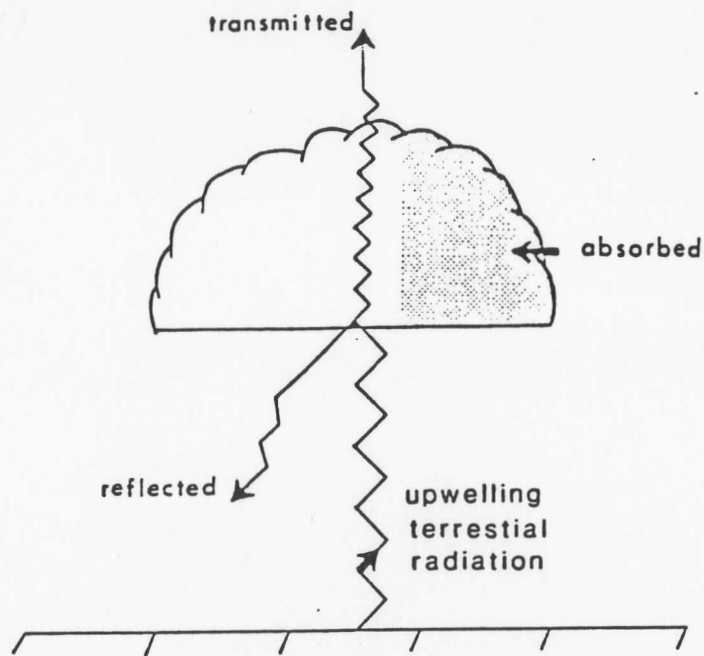


Figure 4: Schematic depiction of the conservation of energy principle.

radiation would be transmitted to space at that wavelength. Such a spectral interval is called a window region. In this case the three parameters governing the radiance are given by

$$a(\lambda) = r(\lambda) = 0$$

$$\tau(\lambda) = 1 \quad . \quad (6)$$

Alternately, if the transmittance is zero, radiation is either absorbed or reflected. In such a case, the albedo or reflectivity (r) of a surface is given by

$$r(\lambda) = 1 - a(\lambda) \quad .$$

Kirchhoff's law, another fundamental relationship in radiative transfer theory which states that the absorptivity of matter is equal to its emissivity, is expressed by

$$a(\lambda) = \epsilon(\lambda),$$

where $\epsilon(\lambda)$ is the emissivity at a given wavelength. Thus, matter which is a strong absorber at a particular wavelength is also a strong emitter at that wavelength. Likewise a weak absorber is also a weak emitter. Since the absorptivity of a blackbody is unity, the emissivity of a blackbody is also equal to unity.

Atmospheric absorption or emission of radiation varies with wavelength. Where atmospheric absorption is strong, little or no radiation from the lower atmosphere reaches space. In regions of the spectrum where very little atmospheric absorption occurs the radiation beam tends to be unattenuated as it propagates from the surface or the lower atmosphere to space. These effects upon radiation due to the atomic characteristics of atmospheric constituents create differences in absorption/emission spectra from the hypothetical values of a blackbody given by the Planck function. Consequently, the spectral distribution of radiation to space in Fig. 2 contains much more variation than depicted by the smooth Planck function curve. In Fig. 3 the differences between the radiation to space calculated from the Planck function and observed radiation values over a segment of the infrared portion of the spectrum

are quite evident. Note the portion of the spectrum where the actual and blackbody radiation are nearly equal is quite limited.

Satellite sensors measure radiation in regions of the electromagnetic spectrum that contain strong absorption bands associated with certain atmospheric constituents. Two atmospheric absorption bands used in the determination of vertical temperature and moisture profiles are associated with carbon dioxide (CO_2) and water vapor (H_2O). The distribution of radiation to space in Fig. 3 shows that between 5-9 μm a strong H_2O absorption band is present. Above 12 μm CO_2 is a uniformly strong absorber except for a large fluctuation near 15 μm . In the region between 9-12 μm where most terrestrial radiation occurs, absorption of radiation by atmospheric constituents is small. This window region permits approximately 50% of the terrestrial radiation to escape to space. The remaining 50% of the terrestrial radiation being emitted outside the 9-12 μm window region is strongly attenuated by the continuous process of absorption and re-emission due to the effects of H_2O and CO_2 . As such, the pattern of terrestrial radiation being emitted to space is quite variable and leads to local differential cooling in the atmosphere on the order of a few degrees per day. Near the earth's surface and at cloud boundaries the local cooling may be significantly greater. Thus, the differential cooling associated with the variation of clouds and water vapor is of sufficient strength to alter the day to day temperature structure of the free atmosphere by a few degrees. Likewise changes in the CO_2 content of the atmosphere are sufficient to enable significant temperature changes at climatic time scales.

Oxygen is another important absorber of radiation utilized by satellite sensors. Oxygen absorbs radiation in the microwave region of the spectrum. Although the amount of radiation emitted in this region is small, radiation at this wavelength is not attenuated by water vapor or small water droplets. Thus, these microwave measurements in the vicinity of 50-60 GHz can provide information beneath clouds.

Remote soundings of the atmosphere and the earth's surface temperature obtained from satellite sensors are generally based on measurements of outgoing longwave radiation in the spectral intervals discussed above. The temperature of the earth's emitting surface, or skin, is measured by sensing within spectral intervals from a number of window regions. Certain of the absorption bands within the spectrum are particularly favorable for use in constructing the vertical distribution of temperature and moisture. The satellite's radiation measurement within a spectral interval is a result of the concentration of the constituent and the temperature at which the radiation is emitted.

By careful selection of different spectral intervals, radiance data from different levels in the atmosphere are obtained from the differences in attenuation of the radiation by the atmospheric constituent. If the absorption by the constituent is weak, the information to infer atmospheric temperature or water vapor content comes from the lower atmosphere. If the absorption is strong, the information comes from levels higher in the atmosphere. In order to infer a temperature profile by these means, the concentration of the atmospheric constituent that

attenuates the radiation within the spectral interval of observation must be known. Since the carbon dioxide content of the atmosphere is relatively uniform, the gas is a suited constituent for inference of temperature. Once the temperature profile is determined, the concentration of variable constituents, such as water vapor, can be determined from spectral radiance measurements. It is essential that within the spectral interval of the observation the particular constituent dominates in the attenuation of the radiation over all other constituents.

In summary, the relatively transparent window regions of the spectrum permit direct sensing of the radiation emitted from the earth's surface, which in turn allows estimation of the earth's skin temperature. In the spectral region less than $9\ \mu\text{m}$ and greater than $12\ \mu\text{m}$ radiation to space is dependent on the atmospheric composition and temperature. The absorption/emission spectra of several atmospheric constituents provides the means to obtain vertical temperature and moisture profiles. If the vertical distribution of a constituent is known, the attenuation by that variable can be eliminated and the temperature profile can be determined from observations of radiance within several spectral intervals. The temperature distribution is determined from observations sensitive to CO_2 and is independent of the water vapor and other variable constituents. With the temperature profile determined, the radiance observations in other spectral intervals can be used to define the vertical distribution of other constituents such as water vapor, ozone, etc.

VI. RADIATIVE TRANSFER

This section develops radiative transfer relations from the concept of energy conservation and Schwartzchild's equation whereby the radiance emitted from the earth's surface and within the atmosphere is related to the radiance measured by the satellite sensor. After the mathematical relations are developed, a discussion of the remote sensing problem follows.

The basic equation dealing with radiative transfer through a medium is Schwartzchild's equation. For a fixed, thin slab of atmosphere the change in upwelling incident radiation is

$$dI[\lambda, \theta] = [-I(\lambda, \theta) + B(\lambda, T(z))] k(\lambda, z) q(z) \sec\theta \rho(z) dz, \quad (7)$$

where $I(\lambda, \theta)$ is the upwelling monochromatic radiance intensity at wavelength λ and viewing angle θ , $B(\lambda, T(z))$ is the Planck radiance for a given wavelength and temperature T at height z , $k(\lambda)$ is the absorption coefficient of the absorbing gas, $q(z)$ is the mixing ratio of the absorbing gas, and $\rho(z)$ is the atmospheric density. The first term on the right hand side specifies the radiation absorbed within a layer, while the second term is the radiation being emitted. This relationship assumes: i) a plane parallel atmosphere; one in which the radiant energy is emitted vertically upward, perpendicular to the earth's surface and the atmosphere's strata and ii) the atmosphere is in local thermodynamic equilibrium. These conditions imply that atmospheric scattering is isotropic (i.e., uniform in all directions) and the thermodynamic state

of the atmosphere is steady (i.e., $\partial T/\partial t = 0$). In radiation theory the atmosphere is usually considered in local thermodynamic equilibrium up to approximately 60 km. With the hydrostatic equation

$$\frac{\partial p}{\partial z} = -\rho g, \quad (8)$$

Schwartzchild's equation is transformed to isobaric coordinates,

$$dI(\lambda, \theta) = [-I(\lambda, \theta) + B(\lambda, T(p))] k(\lambda, T, p) q(p)/g \sec \theta dp. \quad (9)$$

This form is preferred because the pressure dependency of the transmittance functions is known explicitly. The solution of this first order linear ordinary differential equation is obtained through multiplication by the integration factor,

$$\tau(\lambda, \theta, p) = \exp \left[\frac{-\sec \theta}{g} \int_0^p q(p) k(\lambda, p) dp \right], \quad (10)$$

where $\tau(\lambda, \theta, p)$ is the transmissivity for a particular absorbing constituent. Differentiation yields

$$d\tau(\lambda, \theta, p) = -\frac{-\sec \theta}{g} q(p) k(\lambda, p) \tau(\lambda, \theta, p) dp. \quad (11)$$

If (9) is multiplied by τ and combined with (11), the resulting equation (in abbreviated notation) is simply

$$\tau dI = [-I + B] d\tau \quad (12)$$

or

$$\tau dI + I d\tau = d(I\tau) = B d\tau. \quad (13)$$

Since τ and I are functions of the independent variable p , an integration performed from the earth's surface ($p = p_s$) to any pressure level p is given by

$$\begin{aligned}
 & I(\lambda, \theta, p) \tau(\lambda, \theta, p) - I(\lambda, \theta, p_s) \tau(\lambda, \theta, p_s) \\
 &= \int_{p_s}^p B(\lambda, T(p)) \frac{\partial \tau(\lambda, \theta, p)}{\partial p} dp \quad . \quad (14)
 \end{aligned}$$

The earth's surface is usually considered to be a blackbody; consequently, the surface radiance $I(\lambda, \theta, p_s)$ is set equal to the value of the Planck function $B[\lambda, T(p_s)]$. Thus, (14) becomes

$$I(\lambda, \theta, p) \tau(\lambda, \theta, p) = B[\lambda, T(p_s)] \tau(\lambda, \theta, p_s) + \int_{p_s}^p B[\lambda, T(p)] \frac{\partial \tau(\lambda, \theta, p)}{\partial p} dp \quad . \quad (15)$$

In this expression the upwelling radiation is a function of the surface temperature, the transmittance, the angle of viewing, the mass mixing ratio of the atmospheric constituent and the mass of the atmosphere between the earth's surface and the hydrostatic pressure level p . Since for well mixed gases such as CO_2 the mass mixing ratio has been assumed to be known, the functional dependence on the mixing ratio becomes conditional. In the inference of the temperature profiles from satellite observations, the integration extends over the entire vertical extent of the atmosphere from p_s to p equal to 0. The transmissivity $\tau(\lambda, \theta, p)$ is unity by definition. Also, the viewing angle is usually corrected to correspond to the subsatellite point so that the angular dependency is

removed. In this case, the equation of radiative transfer at the upper boundary of the atmosphere simplifies to the form of the radiative transfer equation used in remote sensing from satellites,

$$I_{\lambda} = B[\lambda, T(p_S)] \tau(\lambda, p_S) + \int_{p_S}^0 B[\lambda, T(p)] [\partial\tau(\lambda, p)/\partial p] dp . \quad (16)$$

The left hand side of the equation is the satellite measurement. The first term on the right hand side is the surface contribution to the total radiance and the second term is the atmospheric contribution throughout the vertical depth of the atmosphere.

The profile of temperature is determined through solution for the Planck radiance profile contained under the integral in (16). Then, using the Planck function, the equivalent blackbody temperature can be determined. If the emission source is assumed to be a blackbody, the actual temperature and the blackbody temperature are equivalent. While this is a valid assumption for the atmosphere in some cases, it is not always valid for determining the emission from the earth's surface. This departure can be a significant source of error if the emissivity of the earth's surface is improperly specified.

The energy received by a satellite sensor results from a stream of terrestrial and atmospheric radiation emitted upward. In order to resolve the source of the energy emitted using the radiative transfer equation, the mass of the atmosphere is divided into thin layers (see schematic in Fig. 5). The integral (16) replaced with summation notation and differentials with finite differences is given by

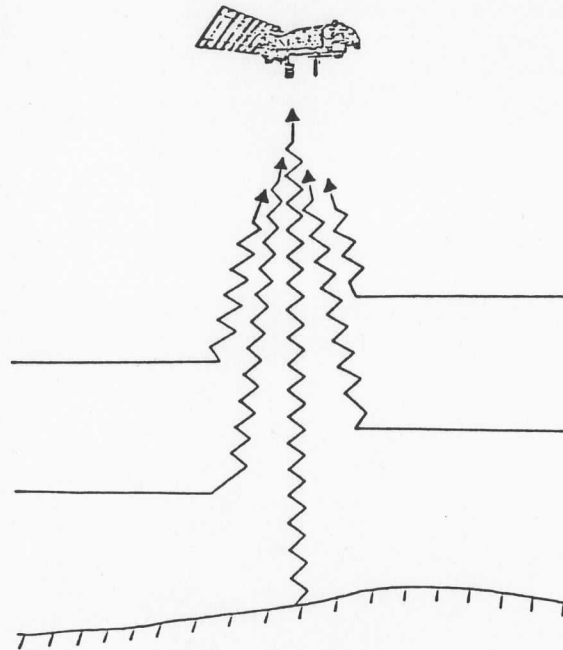


Figure 5: Schematic depiction of the layer approximation to the total energy received at a satellite sensor.

$$I = \epsilon_S B(T_S) \tau_S + \sum_{i=1}^n B(T_i) (\tau_U - \tau_L), \quad (17)$$

where ϵ_S is the emissivity of the earth's surface and the functional dependence of the variables on the wavelength λ is implicit. In this form the atmosphere is divided into n homogeneous layers in which $T(i)$ is the temperature of the i -th layer radiating with intensity $B(T(i))$. The transmittance from the top of the layer to the top of the atmosphere is τ_U , while τ_L is the transmittance from the bottom of the layer to the top of the atmosphere. The total upwelling radiance (I) is determined by the

sum of the Planck radiance (B) contributed from the earth's surface and by a weighted linear combination of the Planck radiance from each of the n layers. The weight within each layer is given by the differences in transmissivity between the top and the bottom of the layer. Soundings produced from satellite data are the highest quality if the summations are carried to the top of the atmosphere (about 1 mb) since the transmittance at the more opaque frequencies varies even to these levels.

The change in transmissivity with respect to pressure ($\partial\tau/\partial p$) in the radiative transfer equation (16) is usually expressed as a weighting function. Less radiation is transmitted directly to space from the lower atmosphere than from the upper atmosphere due to the absorption by various atmospheric constituents. The transmittance/absorption characteristics ($\partial\tau/\partial p$) vary rapidly with the wavelength along the edge of a spectral region of strong absorption (e.g. the $15 \mu\text{m}$ CO_2 band). Such a region is ideal to measure the Planck radiance or brightness temperature in order to determine the temperature of vertical layer of the atmosphere through use of (16). However, since these weighting functions cover a relatively large vertical depth, the vertical resolution of the sounding is somewhat restricted.

The first method suggested by King (1958) and Kaplan (1959) determined atmospheric temperature measurements using angular and spectral radiance measurements, respectively, in the portion of the CO_2 absorption band near $15 \mu\text{m}$ (see Fig. 6). The largest amount of radiation

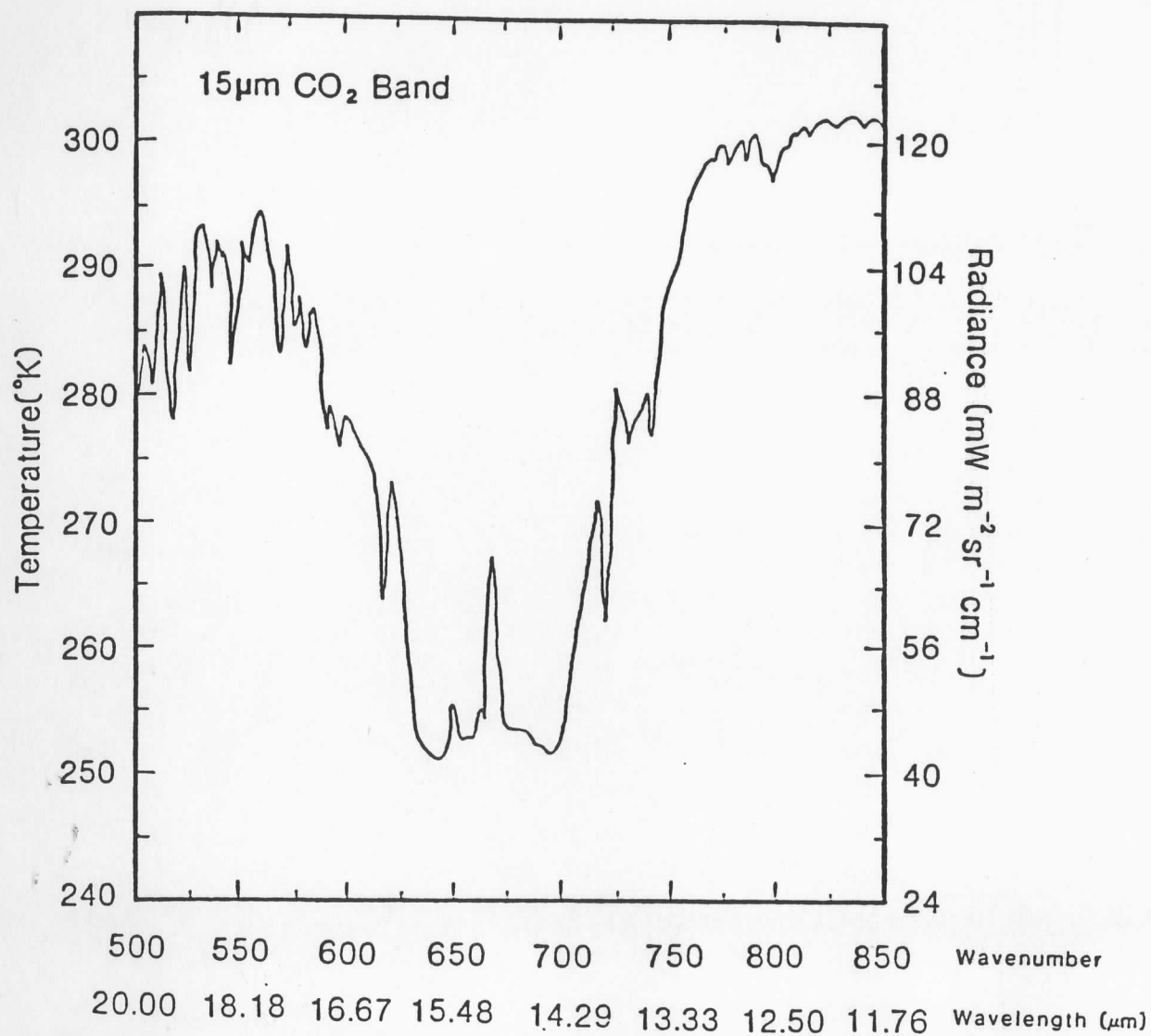


Figure 6: Outgoing radiance in terms of black body temperature in the vicinity of the 15 µm CO₂ absorption band.

is absorbed and re-emitted at the center of the band, characterized by the spike, while weaker absorption occurs towards the edges or wings of the absorption band. Thus, satellite radiance measurements near the band center represent radiation emitted near the top of the atmosphere since emission from below is re-absorbed by upper atmospheric constituents. Measurements in the wings represent radiation emitted from lower atmospheric levels where the upper atmospheric absorption and re-emission is weaker (i.e., the atmosphere is more transparent at this wavelength). Measurement at a number of wavelength intervals provides information at a number of atmospheric levels. This information allows calculation of a vertical temperature profile when the radiative transfer equation at each wavelength is satisfied simultaneously for the measurements at all wavelengths. It is important to note that due to the finite resolution (wavelength bandwidth) of the measurements, overlap of their respective weighting functions often occurs.

In summary, integrating Schwartzchild's equation leads to a solution which determines the total upwelling irradiance received at a satellite sensor from the earth's surface and the atmosphere. Since the energy emitted to space within a specific narrow bandwidth towards the edge or wings of a larger absorption band (e.g., the $15\ \mu\text{m}$ CO_2 band) can be associated with different vertical layers of the atmosphere, radiance measurements from several of these narrow bandwidths can be used to infer the thermal structure of the atmosphere.

VII. LINEARIZATION OF THE RADIATIVE TRANSFER EQUATION

This section discusses the linearization of the radiative transfer equation that is used in several techniques to infer the vertical temperature distribution of the atmosphere. The result is a temperature profile expressed as a matrix that is determined as a linear transformation of the satellite observations through the product of the matrix of weighting coefficients and the matrix of measurements of upwelling radiance.

In terms of the radiation received at a satellite sensor from surface and atmospheric contributions (16), the surface contribution can be determined by sensing radiation from window channels. The atmospheric contribution is then

$$I_{\text{atm}}(\lambda) = \int_{P_s}^0 B[T(p)](\partial\tau[\lambda,p]/\partial p)dp \quad . \quad (18)$$

The derivative of the transmittance with respect to pressure weights the Planck radiance and determines the contribution of an incremental atmospheric layer to the total radiation emitted to space. A first order Taylor series expansion of the brightness temperature yields

$$B = B_0 + \left. \frac{\partial B}{\partial T} \right|_0 (T - T_0) , \quad (19)$$

where 'o' signifies an initial estimate. The difference between the sensor observed radiance and some initial estimate is given by

$$(I - I_0)_{\text{atm}} = \int_{p_s}^0 (T - T_0) \left. \frac{\partial B}{\partial T} \right|_0 \frac{\partial \tau}{\partial (\ln p)} d(\ln p) , \quad (20)$$

where the variable of integration is changed to the logarithm of pressure which tends to be proportional with height. This form is utilized to improve numerical evaluation of the integral. The value of I_0 is calculated from a given temperature profile $T_0(\ln p)$ usually the standard atmosphere, a climatological profile or a forecast temperature field. The term

$$\left. \frac{\partial B}{\partial T} \right|_0 \frac{\partial \tau}{\partial (\ln p)} = W^r(\lambda, p) \quad (21)$$

is defined as the temperature weighting function (Fig. 7). Then for a discrete set of measurements the difference of the radiance associated with a wavelength λ_i is

$$\delta I(\lambda_i) = I(\lambda_i) - I_0(\lambda_i) = \int_{p_s}^0 (T - T_0) W^r(\lambda_i, p) d \ln p . \quad (22)$$

In summation form the difference between the observed and initial estimate of radiance is given by

$$\delta I(i) = \sum_{j=1}^m \delta T_j W^r_{ij}(\Delta \ln p)_j , \quad (23)$$

where $i = 1, 2, \dots, n$ denotes the wavelength λ_i of each channel and $j = 1, 2, \dots, m$ specifies the temperature difference and value of the weighting function $W^r(\lambda_i)$ for each pressure layer, $(\Delta \ln p)_j$.

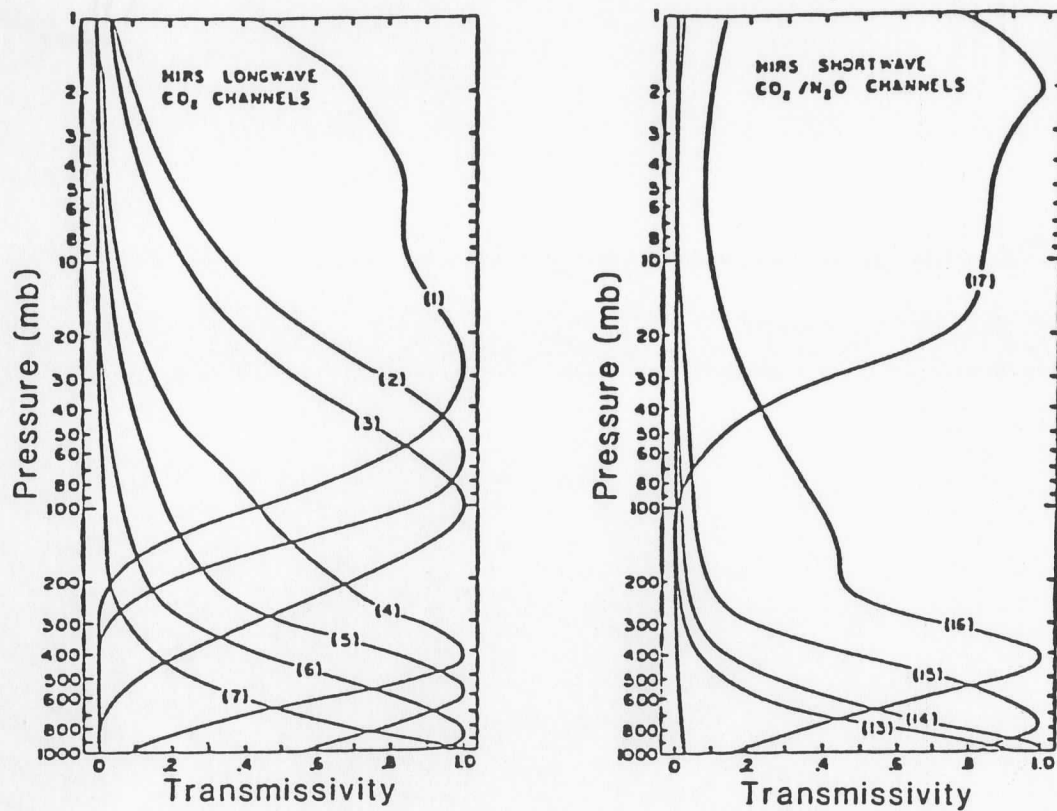


Figure 7: Normalized weighting functions for the High resolution Infrared Radiation Sound (HIRS). Channels 1-7 are located near $15 \mu\text{m}$, channels 13-17 near $4.5 \mu\text{m}$.

With the redefinition of the ij -th weighting function by

$$W_{ij} = W'_{ij} (\Delta \ln p)_j, \quad (24)$$

the differences between the observed and initial estimate of radiance are expressed as an $n \times 1$ vector given by

$$\delta \underline{I}(n \times 1) = \underline{W}(n \times m) \delta \underline{T}(m \times 1), \quad (25)$$

where \underline{W} is the matrix of weights that includes the depth of the layer and $\delta \underline{T}$ is the vector of differences between the temperature to be inferred from the solution and the initial estimates.

In summary, the application of a Taylor series expansion to the radiative transfer equation provides a form which explains the difference between a measured radiance and one expected from an initial guess. The change in brightness temperature with respect to temperature and the change in transmissivity with respect to pressure are combined to define a weighting function in the form of an $n \times m$ matrix through which the problem is reduced to a set of n equations and n unknowns.

VIII. TEMPERATURE PROFILE SOLUTIONS TO THE RADIATIVE TRANSFER EQUATION

The calculation of vertical temperature profiles from a set of measured radiances through the linearized radiative transfer equation requires that (24) be inverted. As previously stated because of the vertical depth of the atmosphere contributing to the outgoing radiation and because of the overlap of adjacent weighting functions, the radiance measurements are not independent of each other. In principle, the solution for this inversion problem is not unique for a finite set of measurements. These factors limit the accuracy of the inverted form of (24) used for remote soundings. Additionally, the exponential

relationship between the Planck radiance and the temperature at infrared wavelengths results in the potential for small errors in the radiance measurement to induce larger errors in the corresponding temperature. Advances in indirect sensing have required that considerable effort be devoted to investigating different methods of solution. Since the limits of accuracy of satellite instrumentation are known and the instruments are constantly being calibrated while in use, the potential for the effects from random errors can be reduced by averaging of repeated measurements.

The two approaches for determining a temperature profile from a set of measured radiances are classified direct and indirect. The direct approach is based on the mathematical inversion of the radiative transfer equation. The indirect approach, which is based on statistical regression relationships between satellite measured radiance values and profiles produced using other data, does not incorporate the radiative transfer equation explicitly. Instead, a statistical regression solution is determined between the large quantity of temperature data already compiled from other sources (radiosondes, balloon measurements, etc.) and satellite measurements coincident with this information.

The direct method of obtaining vertical temperature profiles from a set of measured radiances through (25) is based on the inversion of the known weighting function matrix (\underline{W}) in (24) which with a premultiplication of the inverse (\underline{W}^{-1}) yields

$$\delta \underline{T} = \underline{W}^{-1} \delta \underline{I} \quad . \quad (26)$$

However, the weighting function matrix \underline{W} is nearly singular (the determinant of the matrix is near zero) since the weighting curves at different levels are not linearly independent. Consequently, the inverse method of solution is inherently unstable. This factor plus the inherent noise in the satellite radiance measurements makes the problem of inversion to obtain the atmosphere's temperature by indirect sensing difficult. Initial attempts to utilize the direct method of solution of the radiative transfer equation did not consistently yield accurate temperature profiles.

A number of techniques using the direct method have been devised to calculate temperature profiles through iterative processes. The more noteworthy methods used to obtain remote soundings of atmospheric temperature are summarized below. A brief description of the method of solution is followed by a discussion of the strengths and weaknesses of the technique. The details of the techniques are omitted due to the lengthy mathematical development. The list of references should be consulted for more information concerning a specific method.

SOLUTIONS

A. ITERATIVE METHODS (DIRECT SOLUTION OF THE RADIATIVE TRANSFER EQUATION)

Generally the direct methods of solving the radiative transfer equation iterate or adjust the profile until a better estimate is obtained. Consequently the direct methods usually demand more computer time than an indirect approach based on statistical methods.

One approach developed by Chahine (1968) uses the mean value theorem with a first guess profile in (25) to obtain temperature values at the weighting function peaks. This provides only as many data points as sensor channels from which to construct a profile. If the iteration is not terminated when the convergence criterion is satisfied, the solution will rapidly become unstable. A limitation of this approach is the relatively low resolution of the vertical structure of the atmosphere due to the limitation of one temperature estimate from each channel of information.

Another approach combines the physical direct method with statistical information to obtain temperature profiles. This statistical regularization method (Strand and Westwater, 1968; Turtchin et al., 1970) uses a mean temperature profile from climatology, recent measurement or model forecast and interlevel covariance statistics.

More recent methods of the direct solution incorporate statistical information on the covariance between atmospheric layers to estimate profiles more accurately. These methods involve use of simultaneous

measurements by the satellite and co-located radiosondes (or interpolated values) to adjust the radiance values (Weinreb and Fleming, 1974) or the transmittance functions (Smith et al., 1974; Susskind et al., 1976). The use of statistical methods in this manner renders the direct method very similar to the indirect method. The main problem then becomes one of assembling appropriate statistics.

A technique developed by Smith (1970) for suppression of noise by averaging is based on an iterative direct solution of the radiative transfer equation. This technique does not limit the number of data points. The method uses an initial guess profile but obtains a solution to the atmospheric temperature profile by using a weighted average of the independent estimates of temperature that in actuality are a weighted average of the radiance measurements from several satellite observations. A desirable attribute of this method is the minimization of random instrument noise by the averaging process. However, this technique tends to produce an overly smoothed representation of the vertical temperature structure. Recent refinements (Smith, 1983) have added a direct analytical least-squares technique to the smooth profile to enhance the vertical structure and to provide close agreement between observed and calculated radiances.

B. MATRIX METHODS (INDIRECT SOLUTION OF THE RADIATIVE TRANSFER EQUATION)

Indirect solutions for temperature profiles use the statistical application of discriminant and/or regression analysis without any direct

use of the physical principles involved in the solution of the radiative transfer equation. Most methods use a dependent sample of satellite radiance measurements over a region with a known temperature profile (e.g., from radiosondes) based on prior information and the current radiance measurements to produce a "best fit" profile (Smith, et al., 1970, 1972, 1976; Strand and Westwater, 1968; Rodgers, 1965; Turtchin and Nozik, 1969; Twomey, 1963, 1965). The main problem with the indirect approach is the uncertainty over the representativeness of the dependent sample with respect to location and current time. To partially reduce this problem, different dependent samples which vary with the season and latitude are used.

1) USE OF BASIS FUNCTIONS: This method uses empirical orthogonal functions (EOF's) which are defined from the eigenvectors of a statistical covariance matrix (Wark and Fleming, 1966; Smith and Woolf, 1976). Since the empirical orthogonal functions are based on the determination of independent degrees of freedom, the total explained variance is the sum of the variances explained by each component function. This method, which incorporates prior information, provides a "detailed profile" from a limited amount of observed data somewhat like defining a probability function for the most likely profile given limitations of relatively coarse resolution inherent in these methods.

2) LEAST SQUARES REGRESSION: This method uses least squares to minimize errors without an explicit determination of the weighting functions. A covariance matrix composed of coefficients provides the

smallest least squares of regression between the satellite observed radiances and the infrared radiances expressed directly by the estimates of temperatures. Stability of the solution with regard to the inherent inversion of an ill conditioned matrix of weighting functions embodied in the statistical method is achieved through use of the covariance matrix. The regression matrix requires radiosonde data, thus the accuracy of the method is dependent upon statistical samples of the atmospheric structure in the sounding region from either prior or current information. A form of the regression method developed by Smith (1970) has been used operationally by the National Weather Service.

3) FULL STATISTICAL: This method, which actually is a combination of direct and indirect methods, uses the measured radiances, two covariance matrices (one an error function), and weighting function values which must be known to great precision (Strand and Westwater, 1968; Rodgers, 1968; Turchin and Nozik, 1969). This solution does not need coincident radiosonde and satellite observations. The result is stable but yields profiles with limited vertical resolution. Instrument noise or inexact weighting functions can distort the profiles.

At this time, the regression method with real data has yielded the best results in the analysis/forecast operations. The regression method produces profiles independent of forecast errors which are consistent with radiosonde information. The general iterative method, using calculated "tuned" transmittances and numerical forecast temperatures, also yields good results. However, the errors tend to be correlated with

the errors in the forecast or initial guess profile. This feature may be a disadvantage in attempting to isolate erroneous predictions in some analysis schemes but may be advantageous to maintaining consistency and increasing temporal resolution of atmosphere phenomena which are "subgrid scale" to scales resolved by information from the operational radiosonde network.

IX. TEMPERATURE PROFILE SOLUTIONS FOR CLOUD COVERED CONDITIONS

Cloud water droplets strongly attenuate infrared radiation. Thus, satellite borne infrared sensors cannot determine temperatures below cloud top level. A number of techniques have been developed to overcome this problem. The most successful method has been to compare radiance values between cloud free and adjacent partly cloudy areas in order to determine the fractional area of cloud conditions within each field of view (McMillin and Dean, 1982; Chahine, 1974; and Smith, 1968, 1974, 1976). Through estimation of the fractional area of cloud cover within each field of view, clear column radiances below cloud top height are calculated. In effect, this method eliminates the influence of clouds in the retrieval of the temperature profiles. Another method to obtain temperature profiles under cloudy, non-precipitating conditions as well as clear areas employs measurements in the microwave region of the spectrum (50-60 GHz). Since microwave radiation is virtually unattenuated by small water droplets, measurements in this portion of the spectrum provide optimum estimates of the temperature profile given the limitations of infrared sensing under cloudy conditions.

In view of the sensitivity of temperature retrievals to errors from cloud contamination within each field of view, the most accurate results are produced when the temperature profiles from a number of contiguous fields of view are processed and averaged to provide a single sounding. The infrared sensing instruments onboard current polar orbiting satellites resolve a circular area 30 km in diameter at the sub-satellite point. Figure 8 shows the scan geometry for two consecutive orbits of the NOAA-7 polar orbiting satellite. The information is processed to include soundings from 9 scan spots across the satellite track and 7 scan spots along it. Thus, up to a total of 63 individual soundings may be processed to produce one atmospheric sounding with a horizontal resolution of 250 km. The problem with this approach is to produce a sounding which represents the atmospheric thermal state over this entire area. If undetected clouds are present, the infrared radiance measurements will be contaminated and constitute a non-homogeneous sample. An average sounding determined under these conditions will not be accurate. This situation is referred to as "the clear column radiance problem." Two basic approaches to its solution are: 1) reject measurements from cloud covered regions and find sufficient cloud free regions within the volume to obtain sufficient numbers of uncontaminated soundings to obtain a representative average sounding or 2) apply physical and mathematical techniques to infer clear column radiances from the contaminated data, estimate temperature profiles from clear and partially cloud covered areas, and then determine an average sounding. Both techniques are used operationally at the present time.

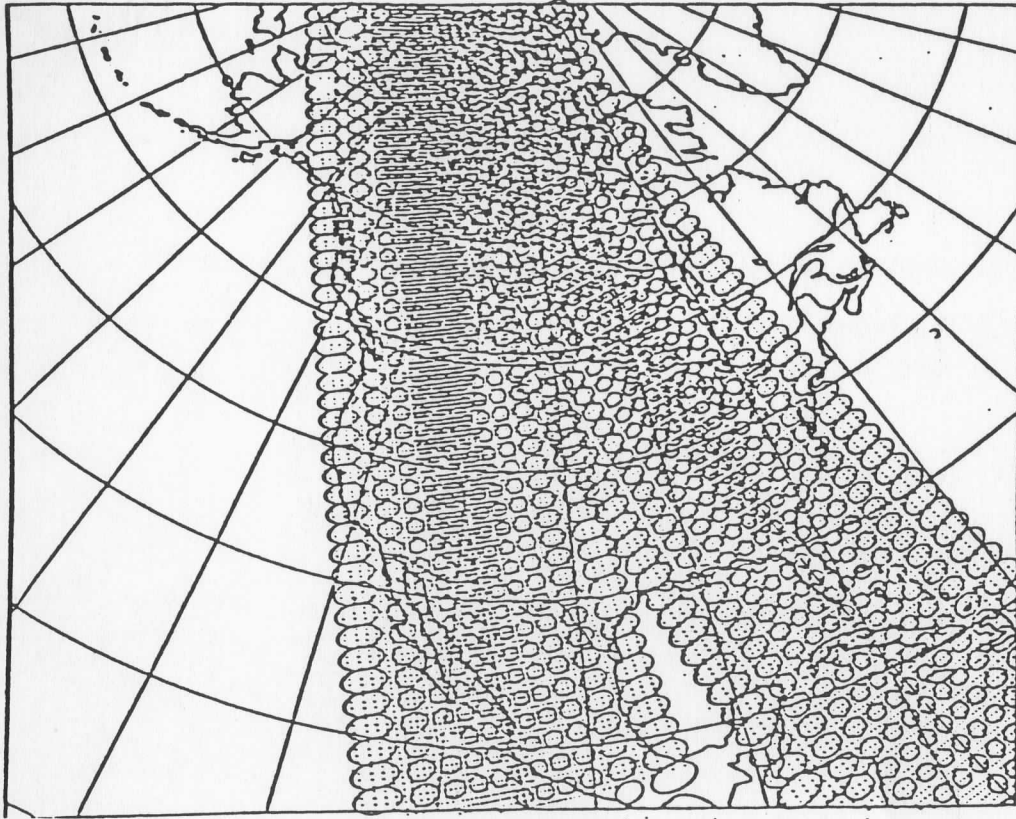


Figure 8: Scan geometry for 2 consecutive passes of the NOAA-6 polar orbiting satellite. Dots represent 30 km HIRS resolution at subsatellite point. Ellipses represent 110 km MSU resolution at subsatellite point.

As the radiance measurements are processed a number of tests are applied to each field of view (FOV) in a given 9x7 box to determine whether or not the FOV is free of clouds. These tests include window

channel radiance comparisons, tests of albedo based on measurements in the visible portion of the spectrum, estimates of surface temperature and a regression comparison of infrared and microwave radiances (Smith et al., 1979). If enough clear FOV's are found, the sounding is obtained from a weighted average of these data. Otherwise, the "adjacent pair" or N* approach is used (Smith et al., 1968, 1974, 1976; Chahine, 1974; Dean, 1982). Limiting factors include simplifying assumptions concerning cloud cover, an independent estimate of the surface temperature and the availability of a high resolution instrument to determine cloud amount. Assuming these factors to be acceptable, the contamination due to clouds is removed and estimates of the clear sky radiance are computed. The adjacent pair approach is subjected to quality control tests similar to those stated for clear sky conditions. However, this technique loses accuracy as conditions approach overcast.

The alternative method of determining the temperature structure below cloud level through scanning microwave spectrometer data leads to a reduction in horizontal and vertical resolution of the infrared atmospheric structure. Due to the lower energy levels of radiation emitted in the microwave region, the spatial resolution of the microwave sounding unit is much less than the high resolution infrared sounder (110 km vs. 30 km). The microwave channels currently used by the NOAA satellites in determining atmospheric profiles are located in the 50-60 GHz region of the spectrum. Weighting functions of the microwave channels are depicted in Fig. 9. Since the upwelling radiance is virtually unattenuated by water vapor or small droplets, the cloud

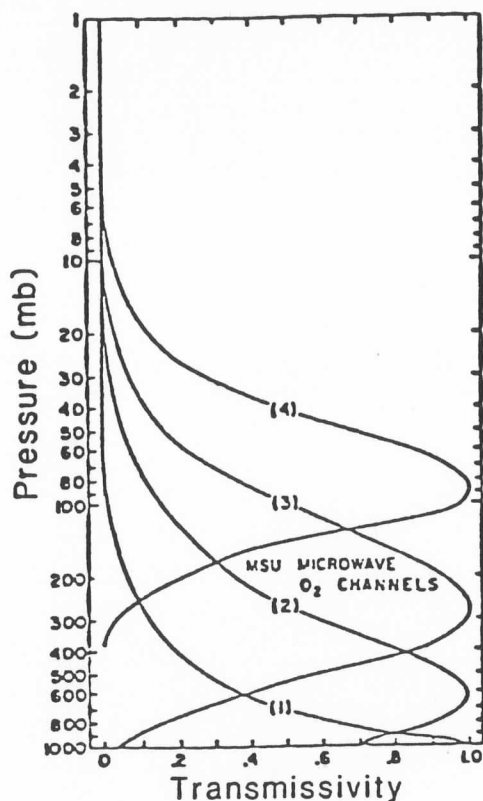


Figure 9: Normalized weighting functions for the microwave Sounding Unit (MSU). Channels 1-4 are located between 50-60GHz.

contamination problem is reduced. However, as precipitation size droplets increase in size, the attenuation of microwave radiation also increases. In the more transparent channels, variations in the surface emissivity must also be considered. Microwave radiance measurements used without other radiance data to estimate vertical profiles will produce very smooth soundings. If, however, infrared and microwave data are used together in cloudy regions, the resultant profiles will have greater detail.

A number of other factors must be considered to obtain accurate calculations of the atmospheric thermal structure.

1) In view of the geometry of satellite scanning radiometers, incoming radiation to the satellite is received at differing path lengths through the atmosphere. These radiance values must be adjusted or normalized to zenith angle measurements.

2) The two major regions of the spectrum utilized in the determination of the thermal structure of the atmosphere are near $4.3 \mu\text{m}$ and $15 \mu\text{m}$. The shorter $4.3 \mu\text{m}$ wavelength band can be contaminated by reflected solar radiation. Thus, measurements in this region must contain a correction for a solar contribution.

3) For channels which are relatively transparent and sense upwelling radiation emitted from the earth's surface, the contribution to the radiance from the earth's surface received at the satellite must be eliminated in order to isolate the atmospheric contribution.

4) Finally, a correction must be made for the surface topography of the earth. Since the terrain extends above sea level, the mass of the atmosphere through which upwelling radiation passes will vary. Thus, the contribution of radiance by layers needs to be altered in retrieval methods to account for the variable mass within an atmospheric column.

X. MOISTURE PROFILE SOLUTIONS TO THE RADIATIVE TRANSFER EQUATION

The radiative transfer equation is also used to estimate total precipitable water or vertical profiles of water vapor. For this solution the temperature profile is assumed to be known (from a

temperature retrieval) while the unknown in the radiative transfer equation is the absorbing constituent, water vapor. Satellite sensor measurements are made near the $6.7 \mu\text{m}$ H_2O absorption band in the infrared region of the spectrum (Fig. 4). Figure 10 shows the temperature weighting functions for the H_2O channels for a typical mid-latitude sounding. Since water vapor is concentrated in the low troposphere and atmospheric gradients of moisture are often large, the retrieval succeeds in recovering only limited details of the actual water vapor distribution. The only water vapor channel which contributes significantly to the total column precipitable water is the one which senses lowest in the atmosphere (channel 11). The use of covariance statistics between atmospheric layers increases the accuracy of water vapor profiles. However, due to the lack of vertical resolution, estimates of the total precipitable water are more reliable than estimates of the profile of water vapor.

Solutions for water vapor profiles from the radiative transfer equation also involve both direct and indirect methods. Indirect statistical solutions utilize coefficient matrices from matched samples of radiance measurements and representative relative humidity profiles (Conrath, 1969; Shen and Smith, 1973). Mixed physical-statistical solutions have been formulated by Shen and Smith (1973) and Weinreb and Crosby (1973). The former iterates a regression equation relating precipitable water to radiance until calculated radiances converge to measured radiances. The latter estimates a mixing ratio profile based on

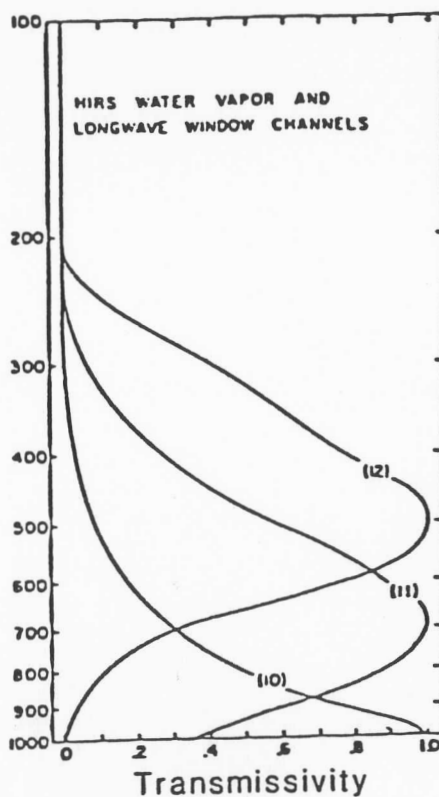


Figure 10: Normalized weighting functions for the HIRS instrument near the $6.7 \mu\text{m}$ water vapor absorption band.

a regression of the temperature profile after which the final solution is determined using empirical orthogonal function analysis.

Direct solutions involve solving the radiative transfer equation by iterative processes. An integration of (16) by parts over the entire vertical extent of the atmosphere yields

$$I_{\lambda} = B[\lambda, T(p=0)] + \int_0^{p_s} \tau(\lambda, p) \frac{\partial B[\lambda, T(p)]}{\partial p} dp \quad . \quad (27)$$

One iterative approach (Smith and Howell, 1971) which approximates the transmittance (τ) by a linear first-order Taylor series expansion is given by

$$\delta I(\lambda)_{\text{atm}} = \int_0^p [u(p) - \hat{u}(p)] \frac{\partial \tau(\lambda, p)}{\partial u} \frac{\partial B(\lambda, T(p))}{\partial p} dp, \quad (28)$$

where δI_{atm} is the difference between the instrument measurement and a radiance calculated from an atmosphere with water vapor path length $u(p)$, defined by

$$u(p) = \frac{1}{g} \int_0^p q(p) dp. \quad (29)$$

The initial estimate, $\hat{u}(p)$, is based on statistics. Iteration of the radiative transfer equation is used to improve estimates of the profile until convergence is reached.

Physical solutions for vertical moisture and temperature profiles are interrelated; that is, accurate estimates of the moisture profile depend on accurate estimates of the temperature profile. Estimates of a temperature profile that is too warm will result in a moisture profile that is too wet, while a temperature profile that is too cold will produce a moisture profile that is too dry. Accurate satellite derived moisture profiles are more difficult to determine than temperature profiles, since in comparison with temperature the radiosonde determined moisture profiles are less accurate while the relative variability of

water vapor is greater. Additionally, most profiles are taken in cloud free regions. This, of course, results in a horizontal bias toward relatively dry soundings. The combined effect of these problems results in RMS errors that are usually in the range of 20-30% (Hayden, 1979). The moisture profiling method used in the VAS (VISSR Atmospheric Sounder; VISSR is an acronym for Visible Infrared Spin Scan Radiometer) research program at the Space Science and Engineering Center uses a technique similar to that used for temperature retrievals. VAS is the instrument package of recently launched geosynchronous (GOES) satellites that measure upwelling radiance with relatively high spatial and temporal resolution. A smooth profile of layer mean relative humidity is obtained using an iterative method technique similar to the above mentioned method of Smith and Howell (1971). Then, a least squares regression of the radiative transfer equation is performed to enhance details of the distribution of precipitable water. Vertical profiles of mixing ratio $q(p)$ or dewpoint can then be calculated using the temperature and moisture data.

XI. CURRENT INSTRUMENTATION FOR VERTICAL SOUNDINGS

Remote sensing of the atmosphere from space is accomplished with two different types of observing platforms, the polar orbiting and the geosynchronous satellite. Polar orbiting satellites move in a pole to pole orbit as the earth rotates beneath it. Through orbital mechanics a sun synchronous polar orbit can be calculated to place the satellite above a given earth latitude at the same local time during each orbit.

The most recently launched polar orbiting satellites, the NOAA series, orbit at an altitude approximately 850 km above the earth's surface with a nodal period of about 100 minutes. This orbital track produces slightly more than 14 orbits per day. Thus, the sub-orbital track does not repeat itself on a daily basis but moves eastward about 3 degrees of longitude per day.

The NOAA series of vertical sounders, TIROS operational vertical sounder (TOVS), combine data from three instruments, the High resolution Infrared Radiation Sounder (HIRS), the Stratospheric Sounding Unit (SSU) and the Microwave Sounding Unit (MSU). The HIRS instrument provides most of the tropospheric sounding data, the SSU provides information from the stratosphere while the MSU is used for vertical temperature profiling in the presence of clouds.

Table 1 shows the bandwidth locations, principal absorbing constituents and levels of peak energy contribution for the various channels of radiation sensing instruments utilized on polar orbiting satellites.

TABLE 1: TOVS INSTRUMENT CHARACTERISTICS

<u>HIRS CHANNEL NUMBER</u>	<u>CENTRAL WAVELENGTH (μm)</u>	<u>PRINCIPAL ABSORBING CONSTITUENT</u>	<u>LEVEL OF PEAK ENERGY CONTRIBUTION</u>
1	15.00	CO ₂	30 mb
2	14.70	CO ₂	60 mb
3	14.50	CO ₂	100 mb
4	14.20	CO ₂	400 mb
5	14.00	CO ₂	600 mb
6	13.70	CO ₂ /H ₂ O	800 mb
7	13.40	CO ₂ /H ₂ O	900 mb
8	11.10	Window	Surface
10	8.30	H ₂ O	900 mb
11	7.30	H ₂ O	700 mb
12	6.70	H ₂ O	500 mb
13	4.57	H ₂ O	1000 mb
14	4.52	H ₂ O	950 mb
15	4.46	CO ₂ /H ₂ O	700 mb
16	4.40	CO ₂ /H ₂ O	400 mb
17	4.24	CO ₂	5 mb
18	4.00	Window	Surface
19	3.70	Window	Surface
20	0.70	Window	Surface

<u>MSU CHANNEL NUMBER</u>	<u>FREQUENCY (GHz)</u>	<u>PRINCIPAL ABSORBING CONSTITUENTS</u>	<u>LEVEL OF PEAK ENERGY CONTRIBUTION</u>
2	53.73	O ₃	700 mb
3	54.96	O ₃	300 mb
4	57.95	O ₃	90 mb

Channels 1-7 of the High resolution Infrared Radiation Sounder (HIRS) are used for temperature soundings. The 15 μm band channels provide better sensitivity to the temperature of relatively cold regions of the atmosphere than can be achieved with the 4.3 μm band channels. A problem of sensing with 4.3 μm channels is the contamination from reflected short wave radiation. Channels 5-7 are also used to calculate the height and amount of cloud cover within the HIRS field of view. Channels 10-12 provide moisture information. The 6.7 μm channel is also used to detect thin cirrus clouds. Channels 13-17, near 4.3 μm , provide better sensitivity to the temperature of relatively warm regions of the atmosphere than can be achieved with the 15 μm band channels because of the exponential relationship of the Planck function at shorter wavelengths. Channels 8 and 18-19 are all window channels used principally to determine surface skin temperature and cloud cover. The combination of 3.7 and 4.0 μm data from channels 18 and 19 enables the reflected solar contribution to be eliminated from observations. The visible channel 20 is used during the day along with the 4.0 and 11.1 μm window channels to define clear fields of view. The Microwave Sounding Unit (MSU) channels 2-4 are also used for temperature soundings. These channels probe through clouds and can be used to alleviate the influence of clouds on the 4.3 and 15 μm sounding channels.

The recently launched geosynchronous (GOES) satellites also carry instrumentation for radiance observations. These satellite orbits lying within the equatorial plane are located approximately 35,000 km above the surface of the earth and rotate at the same angular velocity as the earth.

Thus, the satellite remains fixed over the equator at a particular earth longitude. Since the geosynchronous satellites are located at a much greater distance from the earth than the polar orbiters, measurement accuracy becomes more difficult. Through the central limit effect measurement accuracy is improved by obtaining from the same detector multiple samples of upwelling radiance within a given spectral band. The averaging inherent in multiple sampling increases the signal to noise ratio necessary for consistent estimation of temperature and moisture profiles. Spatial averaging of a number of observations is also employed to improve sounding accuracy. Continuous instrument calibration is a normal operating procedure. The VAS sounder measures radiance in many of the same spectral regions as the polar orbiting satellites. Table 2 provides VAS instrument characteristics.

TABLE 2: VAS INSTRUMENT CHARACTERISTICS

<u>CHANNEL NUMBER</u>	<u>CENTRAL WAVELENGTH (μm)</u>	<u>PRINCIPAL ABSORBING CONSTITUENT</u>	<u>LEVEL OF PEAK ENERGY CONTRIBUTION</u>
1	14.71	CO ₂	40 mb
2	14.45	CO ₂	70 mb
3	14.23	CO ₂	150 mb
4	13.99	CO ₂	450 mb
5	13.31	CO ₂	950 mb
6	4.52	CO ₂	850 mb
7	4.44	CO ₂	500 mb
8	12.67	H ₂ O	surface
9	7.25	H ₂ O	600 mb
10	6.73	H ₂ O	400 mb
11	11.24	WINDOW	surface
12	3.94	WINDOW	surface

The 15 μm CO_2 region is the primary absorption band utilized for temperature profile measurements. The 4.3 μm CO_2 band provides additional temperature sounding data. The smaller number of temperature sensing channels, as compared to the NOAA sounders, does affect the detail of the vertical profiles, but only marginally. Three water vapor channels provide information for moisture profiles while the window channels are used for surface skin temperature and cloud detection. Microwave channels are not present on geostationary satellites since current instrument technology does not permit accurate radiance measurements for the level of energy sensed in the microwave region at this large distance above the earth's surface. The lack of microwave information does not allow for the estimation of temperature profiles in overcast regions.

XII. VIDEOCASSETTE CASE SUMMARIES

Research activities within the Space Science and Engineering Center (SSEC) and a branch of the National Environmental Satellite, Data and Information Service (NESDIS) at the University of Wisconsin-Madison are responsible for developing techniques and applications for satellite derived information. Using the McIDAS videocomputer, scientists are able to interact with the satellite retrieval profiling algorithm to eliminate erroneous data and/or produce additional soundings in regions of need or interest. They may also control the type of solution for clear, overcast or partly cloudy conditions. Recent research projects have investigated many applications to synoptic and mesoscale meteorology, including LFM model input and tropical cyclone intensity and track forecasting. The

videocassette segment of this module utilizes the capabilities of the McIDAS videocomputer to display examples of research conducted by both SSEC and NESDIS scientists.

Two examples demonstrating the use of satellite derived information are included in this videocassette. They are examples of how satellite derived information is aiding analysis and forecasting. The first case, 26 April 1982, focuses on a severe weather outbreak over the southeastern United States. The increased temporal resolution of the satellite data allows forecasters at the National Severe Storms Forecast Center to monitor changes in the atmospheric structure throughout the day. The second case, 15-16 September 1982, investigates Hurricane Debby during its early hurricane stage. In this case the ability to gain meteorological information over data sparse regions is an obvious advantage in forecasting the movement of hurricanes. With the increased resolution in time and space from satellite observations, the development of new techniques has led to accurate estimates of the central pressure and maximum wind speed in hurricanes and a deep layer mean wind field for storm track forecasting (Velden, Smith, and Mayfield, 1984). Summaries of the cases are presented below.

A. 26 APRIL 1982: A SEVERE WEATHER EVENT OVER THE SOUTHEAST UNITED STATES

The severe weather events of 26 April 1982 in the southeastern United States were associated with a mid-latitude cyclone moving through the region. At 1200 GMT on 26 April a 500 mb trough was located over the Mississippi River Valley (Fig. 11) in conjunction with cold air in the mid troposphere and an upper tropospheric jet streak. The 1800 GMT surface

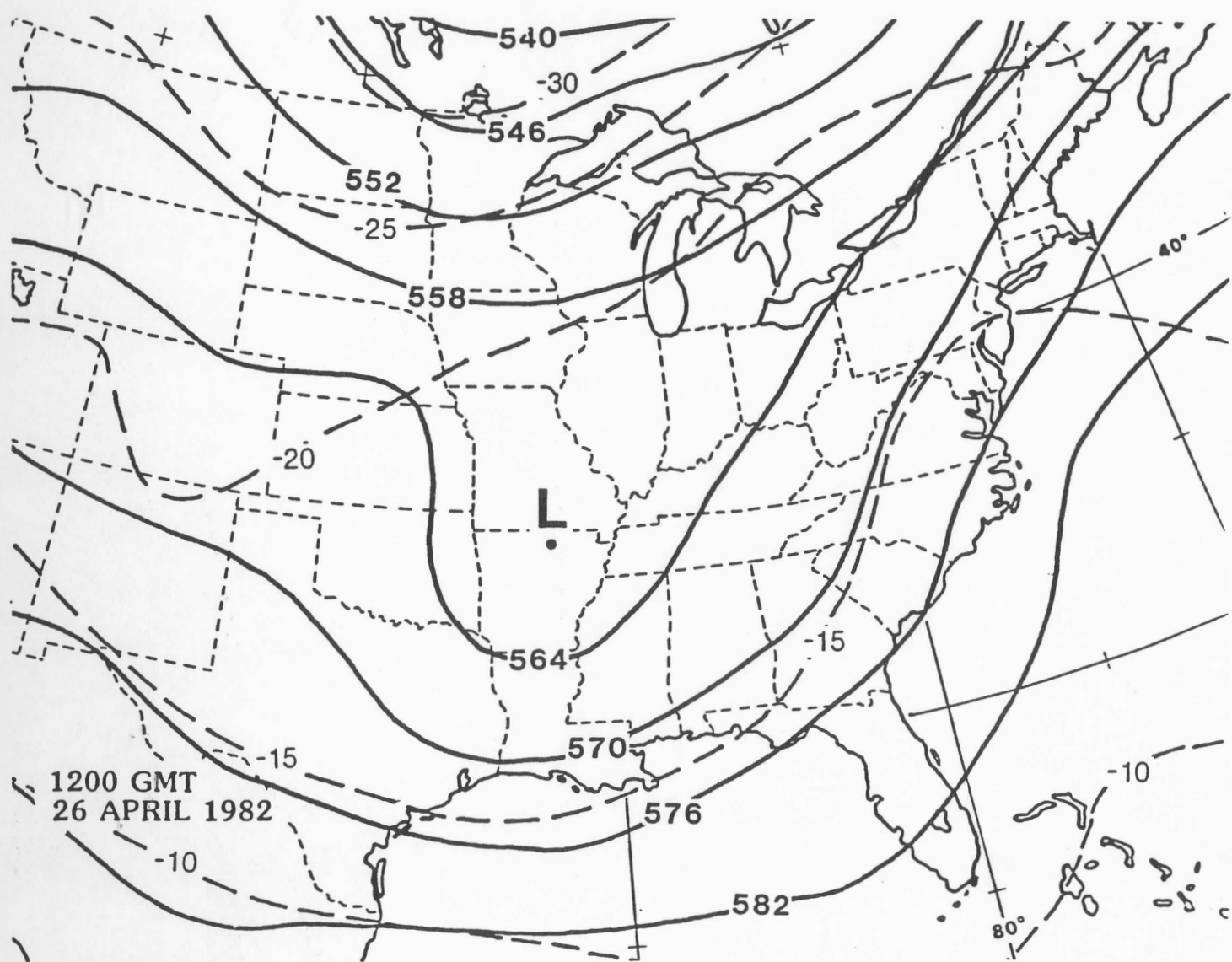


Figure 11: 500 mb geopotential heights (solid lines in decameters) and temperature (dashed lines in °C) for 1200 GMT 26 April 1982.

analysis (Fig. 12) displayed a 1009 mb low in southwestern Tennessee with a frontal boundary stretching through Mississippi. Dewpoints in excess of 15°C (the stipled region) indicate abundant low level moisture. To the west-northwest of the cold front the dewpoint temperatures decrease much more rapidly than the air temperatures. Thus, radiosonde and surface reports from the morning hours of 26 April indicated the potential for strong convection over the Gulf Coast States. Unfortunately, the morning radiosonde data were the last available upper air information until the regularly scheduled releases during the early evening hours.

VAS data from the GOES satellites were available on almost an hourly basis on this day permitting investigation and evaluation of atmosphere structure and evolution throughout the day. Among the important structural changes noted from the VAS temperature and moisture soundings during the day were:

- 1) Rapidly increasing lower tropospheric temperatures due to surface heating in the mostly cloud free region centered over Alabama.
- 2) Increased lower tropospheric total precipitable water due to transport from the Gulf of Mexico.
- 3) Capping by very dry air aloft resulting in increased convective instability over this region.
- 4) Movement of the 500 mb cold air from Arkansas to Tennessee resulting in decreased static stability over Alabama.

The combination of these factors, displayed by the VAS Total totals index (Fig. 13) indicates that the region centered over Alabama is rapidly

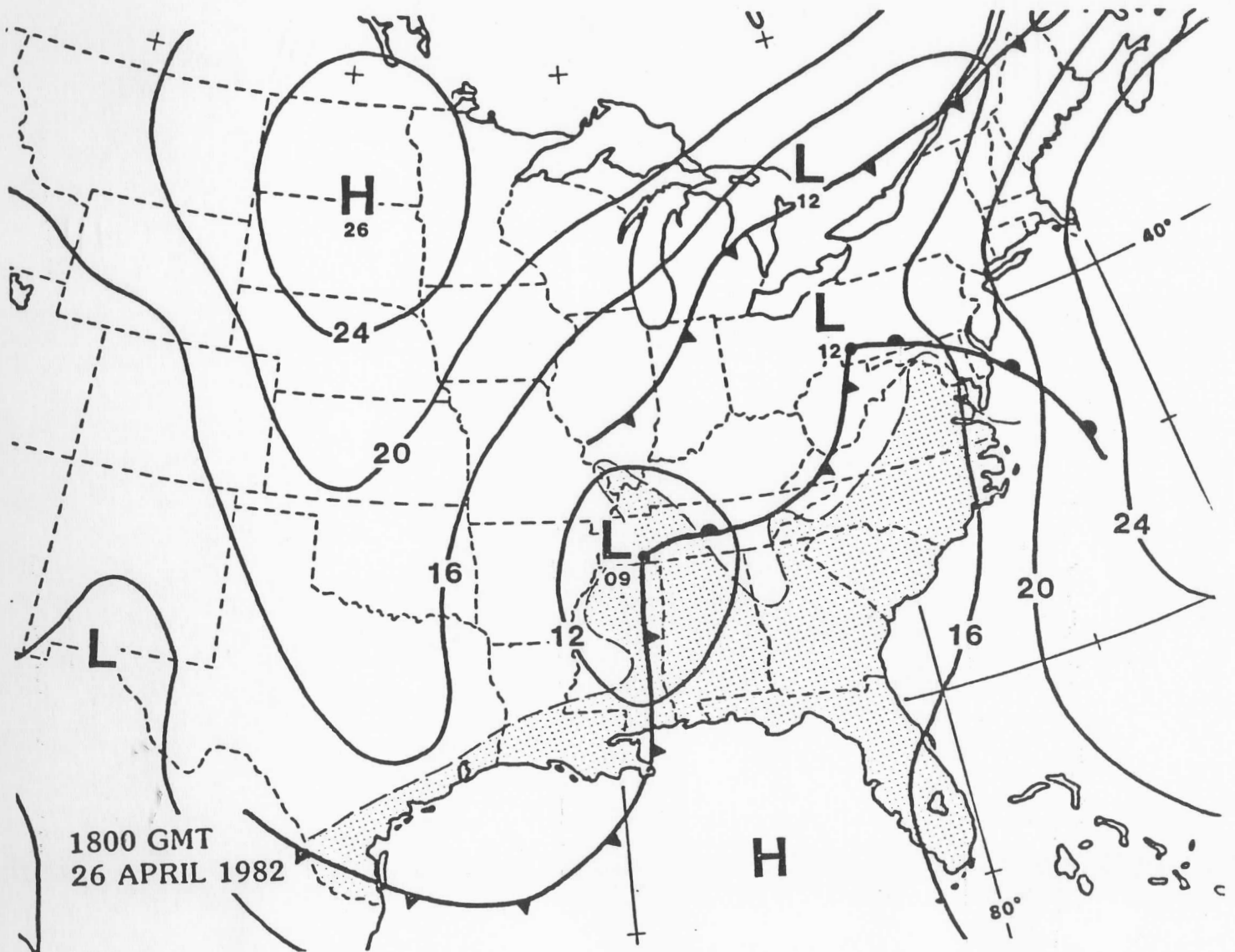


Figure 12: Surface conditions for 1800 GMT 26 April 1982: sea level pressure (solid lines in mb), fronts, and dewpoints (greater than 15°C stipled).

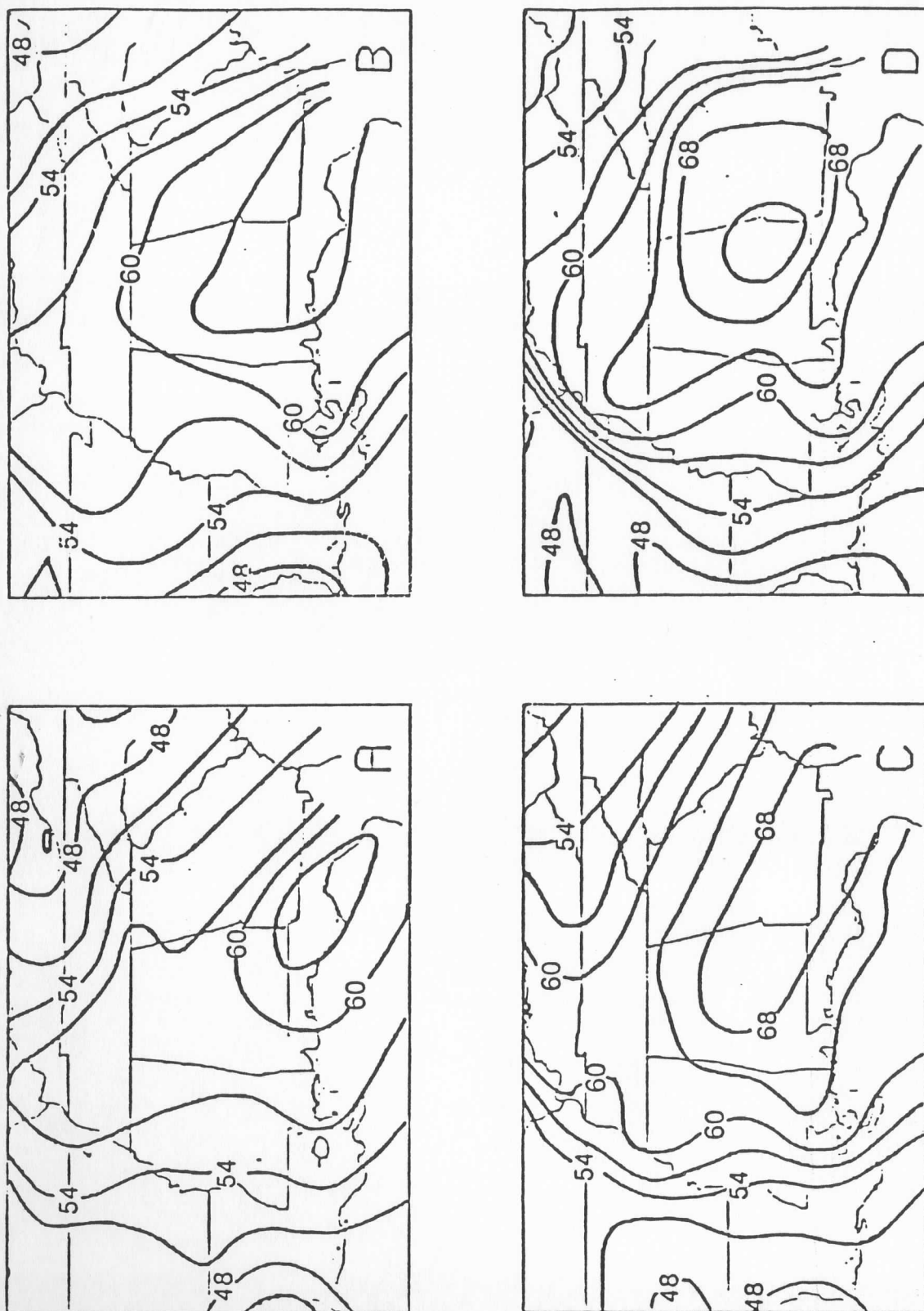


Figure 13: VAS derived Total Totals Stability Index for 26 April 1982
at a) 1600, b) 1700, c) 1900, d) 2000 GMT.

destabilizing with respect to moist convective processes and is becoming a likely location for strong convective development.

The NWS radar summary from 2035 GMT (Fig. 14) indicates numerous thunderstorms in the warm sector of the cyclone and along the frontal boundaries. Four thunderstorms in Alabama had tops in excess of 45,000 feet. Figure 15 shows the location of tornadoes reported on 26 April. Most of these events occurred in the mid to late afternoon.

B. 15-16 SEPTEMBER 1982: HURRICANE DEBBY

The tropical wave that evolved into Hurricane Debby moved off the West African coast on 3 September 1982. Over the next 10 days the easterly wave crossed the Atlantic Ocean with little change in intensity. On 13 September an Air Force reconnaissance discovered a circulation within the system as it passed north of the Dominican Republic and the wave was upgraded to a tropical depression. By 14 September, satellite data indicated the northwestward motion of Debby would be influenced by an eastward propagating mid-latitude trough. The system strengthened quickly, reaching hurricane intensity by the evening of 14 September (Fig. 16). By the early evening of 15 September the central pressure of Hurricane Debby had fallen to 968 mb with winds to 45 ms^{-1} (90 kts) (Fig. 17).

Since very little information is obtained from rawinsonde reports in this area, most of the data available for use in forecasting or as input into models is supplied from satellite derived information. During this tropical cyclone, a special dropwindsonde experiment was conducted by the National Hurricane Research Laboratory to examine the structure of the

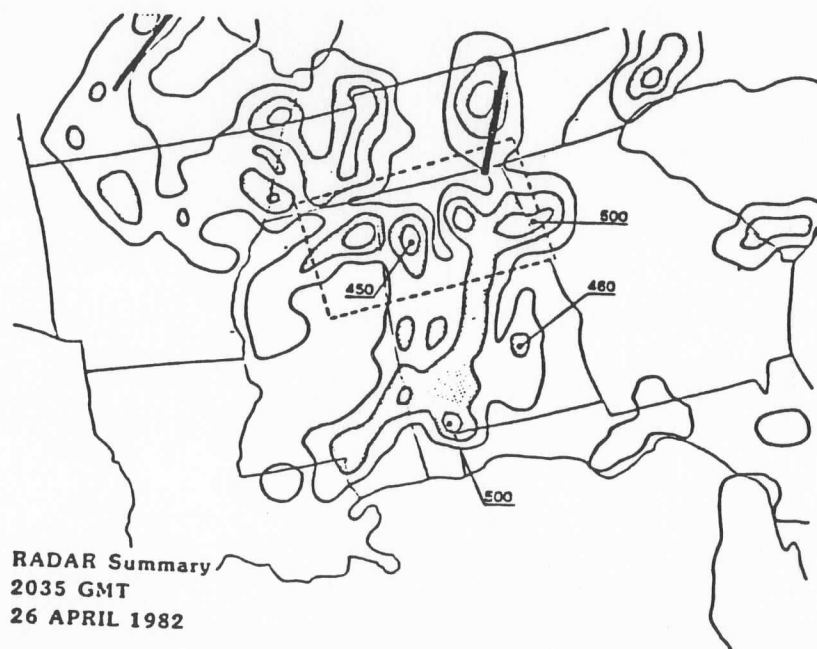


Figure 14: NWS composite radar summary for 2035 GMT 26 April 1982. Contours correspond to rainfall intensity (second level is stippled). Maximum tops are indicated in feet (± 100), squall lines by solid bars, and tornado watch by dashed rectangle.

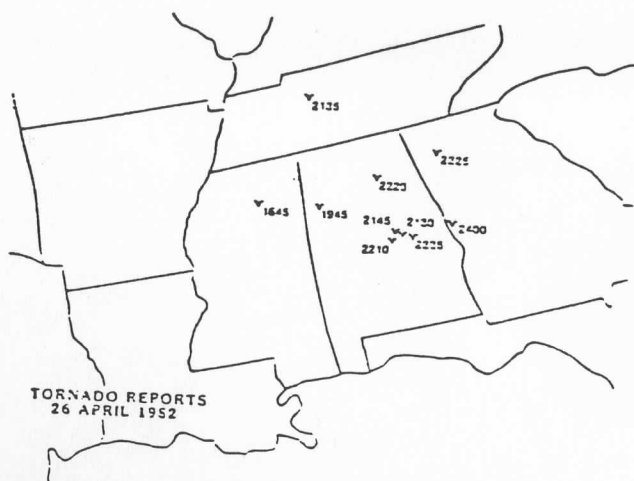


Figure 15: Tornado reports for 26 April 1982 from 1600-2400 GMT. Additional tornadoes were reported in South Carolina in the early hours of 27 April 1982.



Figure 16: Track of Hurricane Debby indicating various stages of development. Location of Debby when videotape shows VAS and TOVS data are also indicated (with storm central pressure and maximum wind speed).

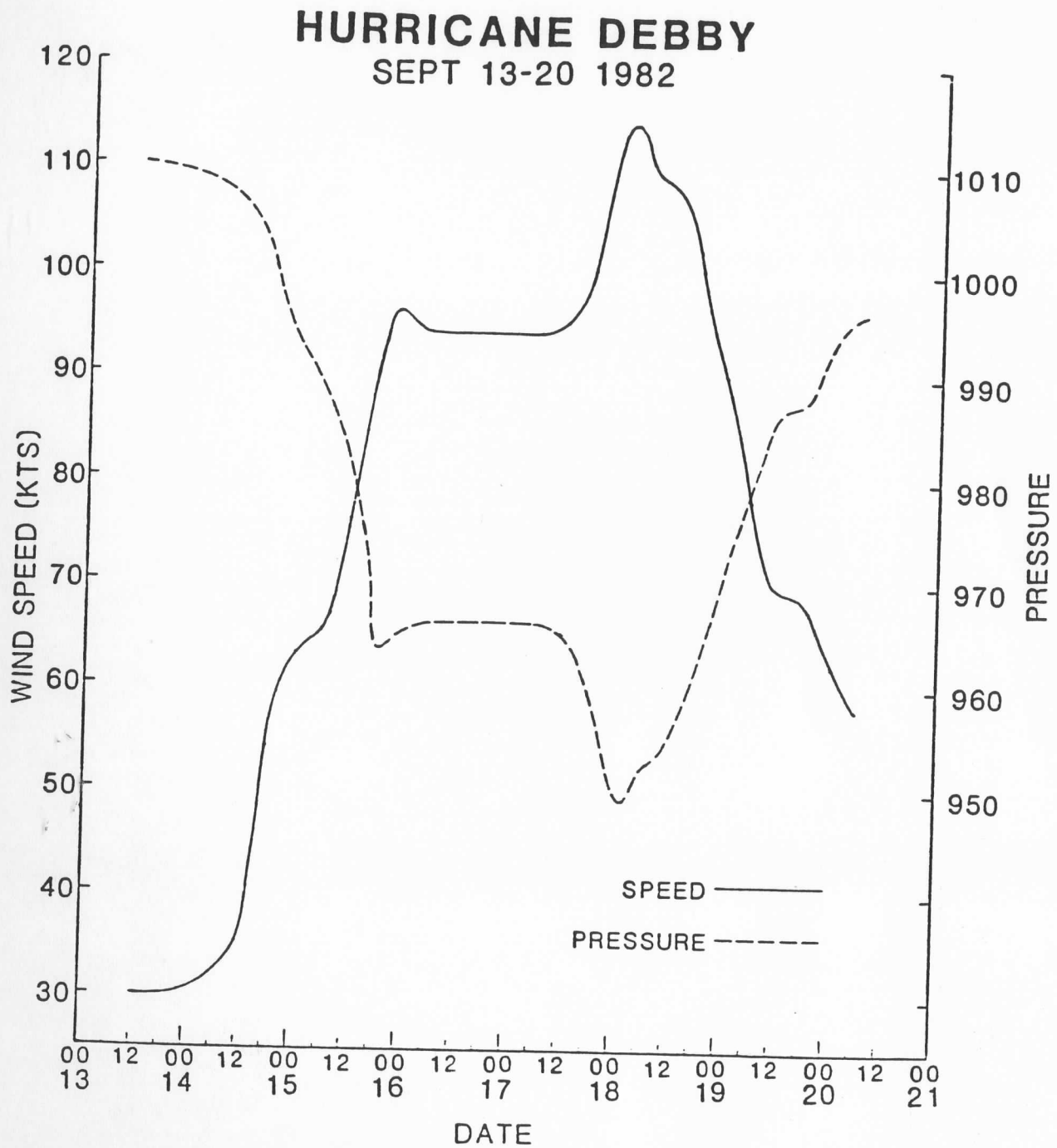


Figure 17: Trace of estimated central pressure and maximum wind speed for Hurricane Debby for 13 September 1982 through 21 September 1982.

environment surrounding the storm. This data provided a means of sounding comparison with the satellite derived temperature and moisture profiles.

VAS temperature and moisture retrievals can provide data coverage over the ocean with excellent temporal and spatial resolution (1 hour in time; 80 km in space). When cloud and water vapor motion wind vectors are added to the data set, a very detailed picture of the atmospheric structure is obtained over regions that previously had almost no available data. Figure 18 shows an example of the VAS coverage.

Hurricane Debby tracked about 130 km to the west of Bermuda on the 16th. Strongest winds reported on Bermuda were near 35 ms^{-1} (70 kts). On the 17th, Debby's forward speed slowed considerably. During the following day a second period of strengthening began as a second mid-latitude trough interacted with the hurricane. Early on the 18th Debby reach its maximum strength with a 949 mb central pressure and peak winds near 60 ms^{-1} (115 kts). As the storm merged with the extratropical system, it accelerated to a forward speed of near 25 ms^{-1} (50 kts) reaching the British Isles on 20 September.

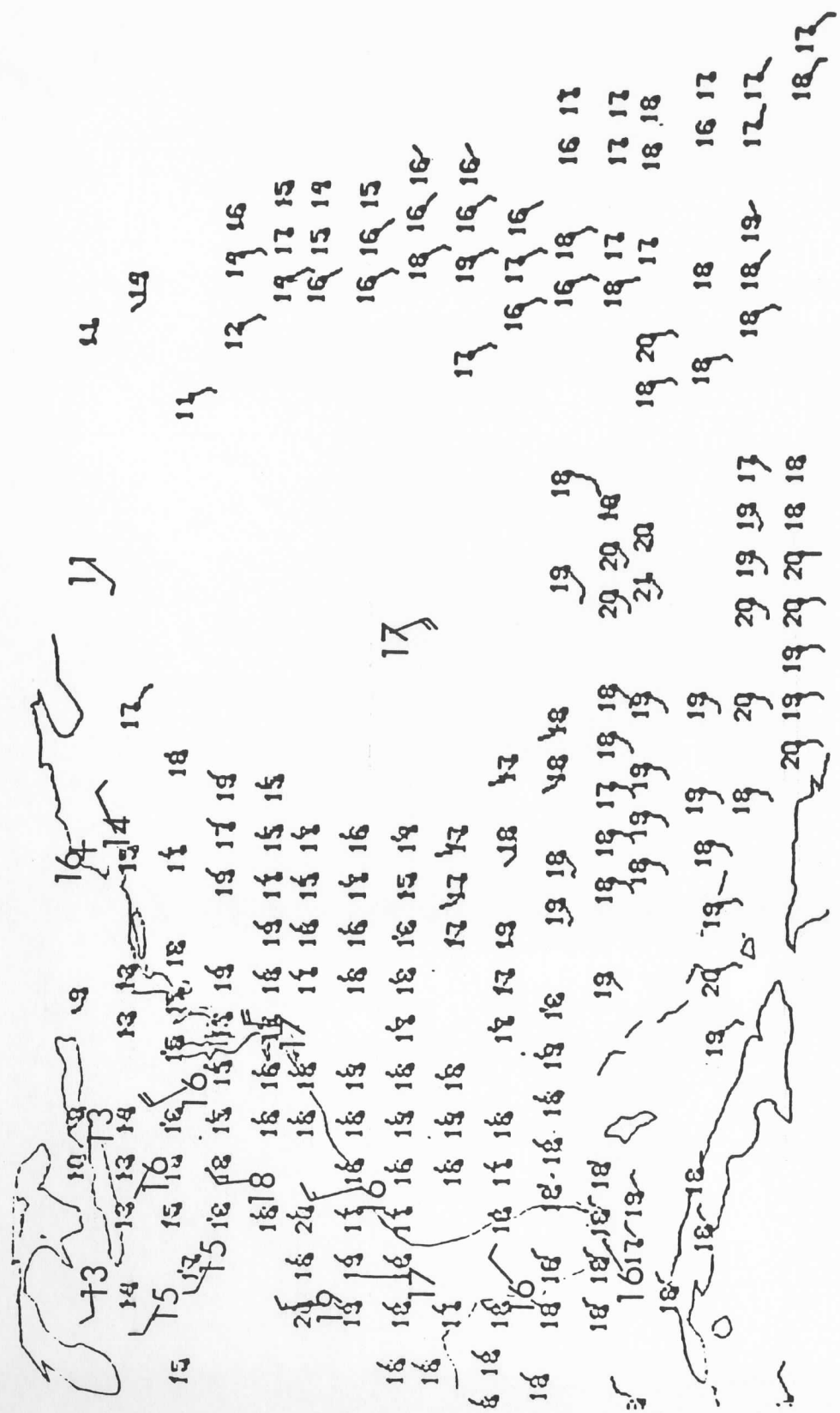


Figure 18: VAS and radiosonde 850 mb temperatures ($^{\circ}\text{C}$) (and winds (ms^{-1}) for 16 September 1982 and 0000 GMT.

ACKNOWLEDGEMENTS

The authors would like to thank Drs. William L. Smith and Christopher M. Hayden of the NOAA/NESDIS Satellite Application Lab, University of Wisconsin-Madison, for their assistance in the manuscript development and also Gary S. Wade and Christopher S. Velden, SSEC - UW-Madison, for their help with the videotape construction.

XIV. REFERENCES

- Chahine, M.T., 1968: Determination of the temperature profile in an atmosphere from its outgoing radiance. J. Optical Soc. Amer., 58, 1634-1637.
- Chahine, M. T., 1970: Inverse problems in radiative transfer: Determination of atmospheric parameters. J. Atmos. Sci., 27, 960-967.
- Chahine, M. T., 1972: A general relaxation method for inverse solution of the full radiative transfer equation. J. Atmos. Sci., 29, 741-747.
- Chahine, M. T., 1974: Remote sounding of cloudy atmospheres, 1. The single cloud layer. J. Atmos. Sci., 31, 233-243.
- Chahine, M. T., 1977: Remote sounding of cloudy atmospheres, II. Multiple cloud formations. J. Atmos. Sci., 34, 744-757.
- Chesters, D., L. W. Uccellini, and A. Mostek, 1982: VISSR Atmospheric Sounder (VAS) simulation experiment for a severe storm environment. Mon. Wea. Rev., 110, 198-216.
- Chesters, D., L. W. Uccellini, and W. Robinson, 1982: Low-level water vapor fields from this VISSR Atmospheric Sounder (VAS) "split window" channels at 11 and 12 microns. NASA TM 83951 (available from NTIS #82N32914, Washington, D.C.).
- Conrath, B. J., 1969: On the estimation of relative humidity profiles from medium resolution infrared spectra obtained from a satellite. J. Geophys. Res., 74, 3347-3361.
- Conrath, B. J., 1972: Vertical resolution of temperature profiles from medium-resolution infrared spectra obtained from a satellite. J. Geophys. Res., 29, 1262-1271.

- Fleming, H. E., and W. L. Smith, 1971: Inversion techniques for remote sensing of atmospheric temperature profiles. Reprint from Fifth Symposium of Temperature, Instrument Society of America, 400 Stranwix Street, Pittsburgh, Pennsylvania, 2239-2250.
- Fleming, H. E., and L. M. McMillin, 1977: Atmospheric transmittance of an absorbing gas 2: a computationally fast and accurate transmittance model for slant paths at different zenith angles. Appl. Optics, 16, 1366-1370.
- Fritz, S., D. Q. Wark, H. E. Fleming, W. L. Smith, H. Jacobowitz, D. T. Hilleary, and J. C. Alishouse, 1972: Temperature sounding from satellites. U.S. Department of Commerce, National Oceanic and Atmospheric Administration, National Environmental Satellite Service, Washington, D.C., NOAA Tech. Rep. NESS 59, 49 pp.
- Hayden, C. M., 1976: The use of the radiosonde in deriving temperature soundings from the Nimbus and NOAA satellite data. NOAA Technical Memorandum, NESS 76, Washington, D.C., 19 pp.
- Hayden, C. M., L. F. Hubert, E. P. McClain, and R. S. Seaman, 1979: Quantitative meteorological data from satellites. Chapter 3, Technical Note No. 166, WMO No. 531, World Meteorological Organization, Geneva, Switzerland, 60-86.
- Hayden, C. M., W. L. Smith, and H. M. Woolf, 1981: Determination of moisture from NOAA polar orbiting satellite sounding radiances. J. Appl. Meteor., 20, 450-466.
- Hunt, G. E., 1973: Radiative properties of terrestrial clouds at visible and infrared thermal window wavelengths. Quart. J. Roy. Meteor. Soc., 99, 346-369.

- Kaplan, L. D., 1959: Inference of atmospheric structure from remote radiation measurements. J. Optical Soc. Amer., 49, 1004-1007.
- Kaplan, L. D., 1961: The spectroscope as a tool for atmospheric sounding by satellites. J. of Quant. Spectrosc. Radiation Transfer, 1, 89.
- King, J. I. F., 1956: The radiative heat transfer of planet earth. In Scientific Use of Earth Satellites, University of Michigan Press, Ann Arbor, Michigan, pp. 133-136.
- King, J. I. F., 1958: The radiative heat transfer of planet Earth. Scientific uses of Earth satellites, 2nd revised edition, J. A. Van Allen (ed.), University of Michigan Press, Ann Arbor, Michigan, 1958, 316 pp.
- Kondratjev, K. Ja. and Timofeev, U. M., 1970: Temperature sounding of the atmosphere from satellites. Hydrometeoizdat, Leningrad, USSR, 410 pp. (Russian).
- McMillin, L. M., D. Q. Wark, J. M. Siomkajlo, P. G. Abel, A. Werbowetzki, L. A. Lauritson, J. A. Pritchard, D. S. Crosby, H. M. Woolf, R. C. Luebbe, M. P. Weinreb, H. E. Fleming, F. E. Bittner, and C. M. Hayden, 1973: Satellite infrared soundings from NOAA Spacecraft. U.S. Department of Commerce, National Oceanic and Atmospheric Administration, National Environmental Satellite Service, Washington, D.C., NOAA Technical Report NESS 65, 112 pp.
- McMillin, L. M., and H. E. Fleming, 1976: Atmospheric transmittance of an absorbing gas: a computationally fast and accurate transmittance model for absorbing gases with constant mixing ratios in inhomogeneous atmospheres. Appl. Optics, 15, 358-363.

- McMillin, L. M., and C. Dean, 1982: Evaluation of a new operational technique for producing clear radiances. J. Appl. Meteor., 12, 1005-1014.
- Phillips, N. A., L. M. McMillin, D. Wark, and A. Gruber, 1979: An evaluation of early operational temperature soundings from TIROS-N. Bull. Amer. Meteor. Soc., 60, 1188-1197.
- Pokrovskiy, O. M., 1969: Optimal conditions for indirect atmospheric sounding. Izv. Acad. Sci. USSR Atmos. Oceanic Phys., 5, 766.
- Pokrovskiy, O. M., 1972: Optimum conditions for indirect sounding of the atmosphere. Izv. Acad. Sci. USSR Atmos. Oceanic Phys., 8, 634.
- Pokrovskiy, O. M., and Yu. M. Timofeyev, 1971: The information yield in indirect sounding of various layers of the atmosphere. Izv. Acad. Sci. USSR Atmos. Oceanic Phys., 7, 598.
- Rodgers, C. D., 1970: Remote sounding of the atmospheric temperature profile in the presence of cloud. Quart. J. Roy. Meteor. Soc., 96, 654-666.
- Rodgers, C. D., 1971: Some theoretical aspects of remote sounding in the earth's atmosphere. J. Quant. Spectrosc. Radiation Transfer, 11, 767-777.
- Rodgers, C. D., 1976: Retrieval of atmospheric temperature and composition from remote measurements of thermal radiation. Rev. Geophys. and Space Phys., 14, 609-624.
- Rodgers, C. D., 1976: The vertical resolution of remotely sounded temperature profiles with a priori statistics. J. Atmos. Sci., 33, 707-709.

- Smith, W. L., 1967: An iterative method for deducing tropospheric temperature and moisture profiles from satellite radiation measurements. Mon. Wea. Rev., 95, 363-369.
- Smith, W. L., 1968: An improved method for calculating tropospheric temperature and moisture from satellite radiometer measurements. Mon. Wea. Rev., 96, 387-396.
- Smith, W. L., 1970: Iterative solution of the radiative transfer equation for temperature and absorbing gas profiles of an atmosphere. Appl. Optics, 9, 1993-1999.
- Smith, W. L., H. M. Woolf, and W. J. Jacob, 1970: A regression method for obtaining real-time temperature and geopotential height profiles from satellite spectrometer measurements and its application to Nimbus-3 SIRS observations. Mon. Wea. Rev. 98, 582-603.
- Smith, W. L., and H. B. Howell, 1971: Vertical distribution of atmospheric water vapor from satellite infrared spectrometer measurements. J. Appl. Meteor., 10, 1026-1034.
- Smith, W. L., H. M. Woolf, and H. E. Fleming, 1972: Retrieval of atmospheric temperature profiles from satellite measurements for dynamical forecasting. J. Appl. Meteor. 11, 113-122.
- Smith, W. L., H. M. Woolf, P. G. Abel, C. M. Haden, M. Chalfant, and N. Grody, 1974: Nimbus-5 sounder data processing system part I: measurement characteristics and data reduction procedures. Final report for GARP Project Office, NASA Contract S-70249-AG, NOAA Technical Memorandum NESS 57, 99 pp., (Available from NTIS, Springfield, Virginia).

- Smith, W. L., P. G. Abel, H. M. Woolf, H. W. McCulloch, and G. J. Johnson, 1975: The High-resolution Infrared Radiation Sounder (HIRS) experiment. Nimbus-6 User's Guide, Goddard Space Flight Center, Greenbelt, Maryland, 20771.
- Smith, W. L., and H. M. Woolf, 1976: The use of eigenvectors of statistical covariance matrices for interpreting satellite sounding radiometer observations. J. Atmos. Sci., 33, 1127-1140.
- Smith, W. L., C. M. Hayden, H. M. Woolf, H. B. Howell, and F. W. Nagle, 1978: Interactive processing of TIROS-N sounding data. Preprints, Conference on Weather Forecasting and Analysis and Aviation Meteorology (Silver Spring, Maryland), American Meteorological Society, Boston, pp. 390-395.
- Smith, W. L., H. M. Wolf, C. M. Hayden, D. Q. Wark, and L. M. McMillin, 1979: The TIROS-N operational vertical sounder. Bull. Amer. Meteor. Soc. 60, 1177-1187.
- Smith, W. L., H. B. Howell, and H. M. Woolf, 1979: The use of interferometric radiance measurements for sounding the atmosphere. J. Atmos. Sci., 36, 566-575.
- Smith, W. L., C. M. Hayden, H. M. Woolf, and F. G. Nagle, 1979: Man-machine interactive processing of satellite sounding data, Submitted to Bull. Amer. Meteor. Soc.
- Smith, W. L., V. E. Suomi, W. P. Menzel, H. M. Woolf, L. A. Sromovsky, H. E. Revercomb, C. H. Hayden, D. N. Erickson, and F. R. Mosher, 1981: First sounding results from VAS-D. Bull. Amer. Meteor. Soc., 62, 232-236.

- Smith, W. L., V. E. Suomi, F. X. Zhou, and W. P. Menzel, 1982: Nowcasting applications of geostationary satellite atmospheric sounding data. Published in Nowcasting, K. A. Browning (ed.), Academic Press Inc. (London) Ltd., pp. 123-135.
- Smith, W. L., and F. X. Zhor, 1982: Rapid extraction of layer relative humidity, geopotential thickness, and atmospheric stability from satellite sounding radiometer data. Appl. Optics, 21, 924-928.
- Spänkuch, D., 1975: Variations in accuracy of the indirect method of determining the vertical temperature profile. Meteorologiya i Hidrologiya, 7, 30-35.
- Staelin, D. H., K. F. Kunzi, R. L. Pettyjohn, R. K. L. Poon, R. W. Wilcox, and R. W. Waters, 1976: Remote sensing of atmospheric water vapor and liquid water with the Nimbus-5 microwave spectrometer. J. Appl. Meteor., 15, 1204-1214.
- Strand, O. N., and E. R. Westwater, 1968: Statistical estimation of the numerical solution of a Fredholm integral equation of the first kind. J. Ass. Comput. Mach., 15, 100-114.
- Suomi, V. E., 1958: The radiation balance of the earth from a satellite. Annals of the IGY, Vol. I, pp. 331-340.
- Turchin, V. F., and V. Z. Nozik, 1969: Statistical regularization of the solution of incorrectly posed problems, Izv. Acad. Sci. USSR Atmos. Oceanic Phys., 5, 14.
- Twomey, S., 1966: Indirect measurements of atmospheric temperature profiles from satellites, 2. Mathematical aspects of the inversion problem. Mon. Wea. Rev., 94, 363-366.

- Twomey, S., 1977: An introduction to the mathematics of inversion in remote sensing and indirect measurements. Elsevier, New York.
- Velden, C. S., W. L. Smith, and M. Mayfield, 1984: Applications of VAS and TOVS to tropical cyclones. (Accepted for publication in BAMS, October.)
- Wark, D. Q., 1961: On indirect temperature soundings of the stratosphere from satellites. J. Geophys. Res., 66, 77-82.
- Wark, D. Q., and H. E. Fleming, 1966: Indirect measurements of atmospheric temperature profiles from satellites, 1. Introduction. Mon. Wea. Rev., 94, 351-362.
- Weubrebm N. P., 1973: Estimation of atmospheric moisture profiles from satellite measurements by a combination of linear and non-linear methods. Third Conference on Probability and Statistics in Atmospheric Science, Boulder, Colorado, June 19-22, 231-235.
- Weinreb, M. P., and D. S. Crosby, 1972: Optimization of spectral intervals for remote sensing of atmospheric temperature profiles. Remote Sensing of the Environment, 2, 193-201.
- Weinreb, M. P. and H. E. Fleming, 1974: Empirical radiance corrections: A technique to improve satellite soundings of atmospheric temperature. Geophysical Research Letters, 1, 298-300.

Appendix A: MODULE EVALUATION

The utilization of videocomputer technology in educational modules provides an innovative resource capable of enhancing classroom instruction. An important step in the development of these modules is feedback from instructors and students to evaluate the impact of this educational resource to facilitate improvements in module content and quality. Students are requested to evaluate this module using copies of the enclosed questionnaire. The instructor is requested to enclose a summary of how the module was utilized, the student's impression of its effects upon the course work and suggestions for improvement. Input from previous module utilization within the Department of Meteorology at the University of Wisconsin-Madison has led to revisions in the videocassette.

A. INSTRUCTOR EVALUATION FOR VERTICAL TEMPERATURE AND MOISTURE PROFILES FROM SATELLITE RADIANCE MEASUREMENTS

In the development of educational modules a critique by faculty and students who have used the materials is essential. A student questionnaire is included in each module package. Student response will aid in modifications of the module being tested as well as help in future module development. A thorough instructor critique of the module is also indispensable. Therefore, faculty members involved in the utilization of the module are urged to complete this questionnaire and offer other comments that would make the module more effective.

Part I Summary

Please evaluate each of the following module components. Space is provided after each statement to state briefly the basis for your response. More detailed comments are sought in Part II of this questionnaire.

	Ex.	Very Good	Good	Fair	Poor
Videocassette visual quality					
Basis of rating:					

	Ex.	Very Good	Good	Fair	Poor
Thoroughness and usefulness of the images, fields and graphics displayed in the videocassette					
Basis of rating:					

Very

Organization of videocassette materials

Basis of rating:

	Very Ex. Good	Good	Fair	Poor

Overall length of the videocassette

Basis of rating:

Too Long	Long	Just Right	Short	Too Short

Length of individual sequences

Basis of rating:

Too Long	Long	Just Right	Short	Too Short

Quality and usefulness of written material
within the manual

Basis of rating:

	Very Ex. Good	Good	Fair	Poor

Map package and data base quality
(if applicable)

Basis of rating:

	Very Ex. Good	Good	Fair	Poor

Audiotrack (if applicable)

Basis of rating:

	Very Ex. Good	Good	Fair	Poor

Technical guide quality

Basis of rating:

	Very			
Ex.	Good	Good	Fair	Poor

Student evaluation forms

Basis of rating:

	Very			
Ex.	Good	Good	Fair	Poor

Part II Instructor Discussion

- 1) Please discuss how you utilized this module; include a) class description, b) how the module was integrated into the course structure, and c) the amount of classroom time and homework required.

2) In what ways (if any) did the module assist you in achieving your classroom goals? What are the modules weaknesses?

3) How would you change the module to make it more suitable for your needs? Why?

4) Please suggest improvements to:

The manual:

The map package and data base:

The videocassette:

The technical guide:

5) In your judgement does this type of material improve atmospheric science education? If you found the modules to be an improvement, how was the improvement attained (please cite examples)?

6) How important do you feel this type of material will be in the future atmospheric science education?

7) Additional comments.

B. STUDENT EVALUATION FOR VERTICAL TEMPERATURE AND MOISTURE PROFILES
FROM SATELLITE RADIANCE MEASUREMENTS

The module was constructed with the intention to support a series of lectures and additional readings. It can present considerable difficulty if used in too rapid a fashion. Please keep these ideas in mind as you complete the evaluation. This evaluation is intended to judge the effectiveness of the videotape as a teaching tool in atmospheric science. Your answers will help to improve the quality of tapes such as this. Please write a short response in the space provided below. Thank you.

- 1) What was the overall pace of the presentation of the material in the classroom

Fast _____

All right _____

Slow _____

Comments:

- 2) Was the visual quality of the tape acceptable (were you able to distinguish important features)?

Good _____

All right _____

Needs improvement _____ (please state where)

Comments:

- 3) Did the module help you to understand the radiometric sounding process more fully?

If yes, how?

- 4) Please express your opinion with a ✓ that indicates the value of each of the following sections of the videotape in aiding your understanding of the topic.

	Very Helpful	Somewhat Helpful	Knew all the material already	Not Helpful
	_____	_____	_____	_____
I Current operational satellite characteristics				
II Physical basis of remote soundings				
III Satellite instrument characteristics				
IV Solutions to the radiative transfer equation				
V Examples depicting the use of satellite soundings				

Comments:

5) Is there other material you would like to see on this tape?

6) Were there any portions of the videocassette that you feel did not contribute or did not present the material well? Explain.

7) Was the audio track (if used) of value to your understanding of the tape contents?

Yes _____

Somewhat _____

No _____

Comment:

8) Do you think this tape has been an educational aid to the material presented in this class? Why?

9) Any additional comments?

Appendix B: Videocassette Technical Guide

	<u>Time</u>	<u>Counter</u>
Title: Vertical Temperature and Moisture		
Profiles from Satellite Radiance Measurement	1:00	029
Example of radisonde & satellite derived profiles	1:30	044
Spatial and temporal resolution of sounding information	2:54	077
Technical information on meteorological satellites	5:05	131
Geostationary	5:15	135
Polar orbiting	6:32	164
Physical basis of satellite derived atmospheric profiles	7:55	194
Radiation measurement bands and associated weighting functions	15:08	335
Characteristics of VAS radiance measurements	18:01	386
Summary	25:53	481
Characteristics of TOVS microwave radiance measurements	24:50	496
Solution for satellite derived moisture and temperature profiles	26:25	520
Examples of solutions for satellite derived moisture and temperature profiles	27:22	534
Examples depicting the use of satellite data	33:18	618
26 April 1982	33:25	621
15-16 September 1982 - Hurricane Debby	43:12	748
End	52:09	854